Role of Surface Chemistry in Semiconductor Thin Film Processing

J. G. Ekerdt,[†,§] Y.-M. Sun,[‡] A. Szabo,[‡] G. J. Szulczewski,[‡] and J. M. White*[,‡,§]

Departments of Chemical Engineering and of Chemistry and Biochemistry, Center for Materials Chemistry, and Center for Synthesis, Growth, and Analysis of Electronic Materials, University of Texas at Austin, Austin, Texas 78712

Received September 11, 1995 (Revised Manuscript Received April 9, 1996)

Contents

1. Introduction

Microelectronics plays a major role in a host of late twentieth century technologies. Everywhere you look, microprocessors seem to be present. Taking the venerable automobile as one example, the preparation of materials and manufacture of components involve machinery controlled by microprocessors, the assembly involves machines with microprocessor "brains", quality is monitored in data-gathering functions with microelectronic devices at many stages, the operating engine itself is steadily monitored and adjusted in real-time using microprocessor-based instruments, when driving we can access, by computers, maps identifying our location and guiding us to our destination, inventories and delivery schedules are kept on computers, and buyers and sellers and lending institutions are all stitched together with such microelectronics equipment. Another example widely heralded today, the "information highway", depends, in the homes and offices of users, on powerful desk top computers that are not only swift and of enormous capacity but relatively inexpensive. Reaching these technological and economic criteria has depended upon exquisite engineering of materials and device structures and machines based on them, along with elegant software.

Underlying these technological and engineering marvels are a large number of fascinating, and not thoroughly understood, fundamental issues that involve solid state and interface chemistry and physics. The acronyms assigned to processes used to prepare electronic materials and devices often point toward the importance of the chemistry involved. For example, CVD and MOCVD, denoting chemical vapor deposition and metalloorganic chemical vapor deposition, respectively, are widely used in microelectronics manufacturing, and both involve, often complex, chemical reactions at and just above growing interfaces. Historically, research chemists have often become actively involved as industrial professionals, but basic research into the chemistry of these important materials and processes has more recently become active in academic halls.

The materials themselves are of considerable interest. In today's market, while silicon lies at the core of most microelectronics technologies and is relatively mature, the controlled preparation of many other materials is a great challenge, especially films and structures with very small feature sizes. Outstanding among the non-silicon electronic materials is optoelectronics and photonics, which, as the name suggests, involves optically active materials that emit or detect light. Compound semiconductors built from elements of columns 13 and 15 (III−V) or columns 12 and 16 (II−VI) are of great interest here, particularly as light emitters, e.g., light-emitting diodes and solid state lasers. Examples are GaAs from the III−V arena and ZnSe from the II−VI group. Their compound character often introduces formidable challenges associated with stoichiometric control, challenges that are obviously absent with elemental semiconductors such as Si. Also *interface* stoichiometry is just as important as, and will likely present different control problems than, bulk stoichiometry. But compared to elemental semiconductors, there are obvious advantages. In particular "bandgap engineering" in which the wavelength emitted is tuned by selecting the composition mole fractions, i.e., the stoichiometry, of the various elements used. For example, the successful controlled stoichiometry of mixtures of Al, Ga, and In with N, P, As, and Sb leads to materials of controlled color for lighting and display applications as light-emitting diodes. These ultramodern light bulbs, containing no filaments, convert electrical to optical energy up to 10-fold more efficiently than conventional filament-based bulbs. Because they contain no filaments, their lifetime is also much longer than conventional bulbs. Achieving the required stoichiometric control is an ongoing challenge and one addressable by chemists.

Many materials besides Si and its oxides are involved in modern silicon-based microelectronics,

* Corresponding author. Phone: (512) 471-3704. Fax: 471-9495. E-mail: jmwhite@mail.utexas.edu.
† Department of Chemical Engineering.
‡ Department of Chemistry and Biochemistry.
§ Center for Synthesis, Growth, and Analysis of Electronic Materials.

S0009-2665(95)00236-6 CCC: $25.00

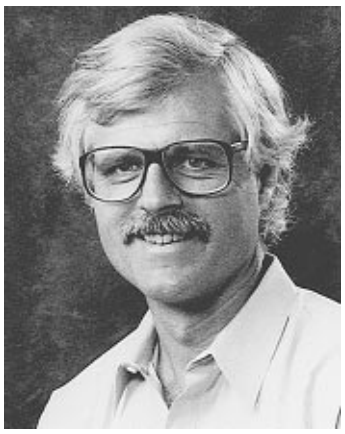

John G. Ekerdt received a B.S. degree from the University of Wisconsin, Madison (1974), and a Ph.D. degree from the University of California, Berkeley (1979). He joined the faculty at the University of Texas at Austin in 1979, where he now holds the Z. D. Bonner Professorship in Chemical Engineering and is the Associate Director of a NSF Science and Technology Center for the Synthesis Growth and Analysis of Electronic Materials. The focus of his research is in the areas of catalytic and surface reaction chemistry and of compound semiconductor and silicon thin film growth and chemistry.

Yangming Sun was born in Shanghai, The People's Republic of China. He completed his undergraduate degree in chemical engineering in 1964 and his graduate work in 1968, both at Tsinghua University in Beijing. From 1968 to 1978, he worked in the chemical industry. Beginning in 1978, Sun served as a faculty member at Tsinghua University, culminating in his appointment to full professor in 1988. In 1990, he joined the research staff at the University of Texas at Austin, where, in 1992, he accepted a permanent position as Research Associate in Chemistry. Sun's recent work has focused on nonthermally driven reactions, precursor chemistry on silicon and III–V semiconductor surfaces, and reactions of N-containing molecules on well-characterized transition metal surfaces.

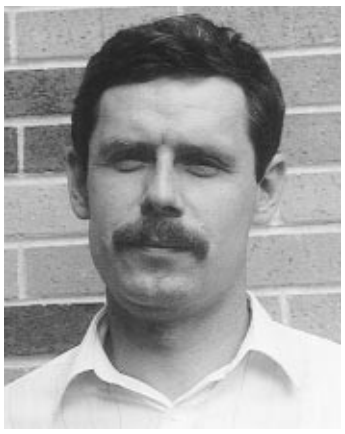

Andras Szabo was born in Miskolc, Hungary, in 1958. He received his diploma in physics from the Roland Eotvos University in 1983. He started graduate studies in 1986 at the Surface Science Center of the University of Pittsburgh under the supervision of Prof. John T. Yates, Jr. During 1991–1993, he did postdoctoral work with Prof. Thomas Engel at the Department of Chemistry of the University of Washington. In 1993, he became a permanent staff member in Prof. John M. White's group at the Department of Chemistry of the University of Texas. During his graduate and postdoctoral research work, he has used numerous experimental techniques, including electron-stimulated desorption, molecular beam techniques, scanning tunneling microscopy, and infrared spectroscopy, for studying surface phenomena on a variety of substrates, which include metal single-crystal, silicon, and metal oxide surfaces. His major interest is in nonthermally stimulated chemical processes.

Gregory J. Szulczewski was born in Detroit, MI, on January 26, 1966. He received his B.S. degree in chemistry from the University of Michigan in 1989 and completed his Ph.D. degree in physical chemistry from Wayne State University in 1995 under the guidance of Dr. Robert J. Levis. His dissertation research included the construction and utilization of a molecular beam apparatus to perform collision-induced reactions of chemisorbed molecules on metal surfaces by energetic, neutral noble gas atoms. Currently, Dr. Szulczewski is a postdoctoral research assistant in the laboratory of Prof. J. M. White at the University of Texas in Austin, where he is studying the dynamics of nonthermal surface reactions stimulated by photons and electrons.

and issues surrounding them are attracting considerable attention. For example, when connecting together the active transistors in ultralarge scale integrated circuits (ULSI), the wiring must scale in length and thickness with the active components in order to fully realize improvements in speed and frequency response. As these length scales are reduced into the deep submicron regime, below 0.25 μm, to realize intrinsically faster transport of charge and, thereby, improved potential device speed, the interconnect and packaging materials may have important impacts. For example, in the manufacture of integrated circuits, barrier layers, e.g., transition metal nitrides, at interfaces between insulators, conductors, and semiconductors are important, and their deposition and thickness control over the microscopically rough terrains encountered in manufacturing is a technologically challenging problem involving surface chemistry.

In this paper, we will review examples drawn from several fronts relevant to electronic materials, the goal being to illustrate the role of surface chemistry in semiconductor processing. We draw on examples from both compound and silicon-based materials systems. Starting with III−V (13−15 in terms of most recent periodic table designations) compound semiconductors in section 2, we focus on GaAs but, for perspective, include some work on nitrides and sulfides of Ga. Thematically, this section focuses on the chemistry of precursor adsorption and decompo-

John M. White was born in Danville, IL, on November 26, 1938. He received a B.S. degree in chemistry from Harding College in 1960 and Ph.D. degree in chemistry from the University of Illinois in 1966. He joined the chemistry faculty at the University of Texas at Austin in 1966 and was named associate professor in 1970 and full professor in 1976. From 1979 to 1984, he served as department chair, and since 1991, he has directed the NSF-supported Science and Technology Center for Synthesis, Growth, and Analysis of Electronic Materials at the University of Texas. White has held the Norman Hackerman Professorship in Chemistry since 1985. He is actively working on problems in surface and materials chemistry, dynamics of surface reactions, and photoassisted surface reactions. The author of over 500 scientific articles, he has served as advisor to more than 50 Ph.D. students.

sition, a topic lying at the heart of 13−15 compound materials film growth. Both thermal and nonthermal, photon and electron, methods of activation are examined. In section 3, we discuss a cross section of processing steps, each involving chemical issues, used in silicon-based device processing. These include the chemistry involved in film growth of semiconductors, dielectrics, barrier materials, and metal interconnects. In semiconductor film growth, the focus is on precursor surface chemistry leading to Si and Ge film growth. For dielectrics we review oxynitride films as the insulator between Si and metal in metal−oxide−semiconductor (MOS) device structures. Barrier and interconnect materials are illustrated using titanium nitride and copper deposition. In addition to these materials issues, we examine, from a chemical perspective, plasma processing, a widely used manufacturing tool where there remain a tremendous number of fundamental issues of nonthermal chemical reactions at and near growing films. Woven into this material dealing with silicon-based technologies, we describe recent developments in the use of novel *in-situ* optical monitoring tools, e.g., femtosecond second-harmonic generation (fs-SHG).

2. 13–15 Compound Semiconductors

This section concentrates on the surface chemistry relevant to thin film growth of GaAs(100) by chemical vapor deposition (CVD) because it is the most widely studied system. In CVD, gaseous sources of the column 13 and 15 elements, either hydrides, organometallic compounds, or adducts, are used to grow thin films. These gaseous sources (or precursors) must dissociatively adsorb, the ligands must desorb or undergo a reaction that leads to a volatile and desorbed product, and the metals must incorporate into the lattice positions, resulting in an epitaxial film. Surface science studies that make use of such common techniques as temperature-programmed desorption (TPD), X-ray photoelectron spectroscopy (XPS), static secondary-ion mass spectroscopy (SSIMS), and high-resolution electron energy loss spectroscopy (HREELS) reveal the reaction mechanisms, reaction energetics, and relative reaction probabilities and permit one to develop chemical kinetic models. These issues are central to understanding and developing CVD processes. We focus on thermal processes since thermal activation of reactants and adsorbates dominates CVD processes. Nonthermal activation, which is required in some situations, is also discussed.

2.1. Alkyl Ligand Reactions

The original CVD processes employed hydride- or chloride-based precursors.[1] Toxicity and corrosion issues directed the search for other precursors and led to the development of CVD processes that employ organometallic precursors featuring trialkyl group 13 compounds (such as trimethyl- or triethylgallium) and group 15 hydrides or organohydrides (such as arsine or *tert*-butylarsine).[1] The group 13 hydrides are unstable and can be used only when present as an adduct, such as trimethylamine allane; even then, the thermal stability is such that film growth uniformity is a persistent problem. Carbon incorporation became an immediate concern and continues to be a problem with the use of organometallic precursors. Some of the relevant questions posed by the use of alkyl ligands are how the alkyl ligands interact with the surface and adsorbed hydride ligands, how the alkyl ligands are removed from the surface, and how carbon is incorporated into the films.

GaAs(100) undergoes several As- and Ga-rich reconstructions,[2,3] and the adsorption and decomposition of organometallics on GaAs(100) is highly dependent on surface structure (for a comprehensive review, see ref 4). In general, the adsorption of alkylgallium precursors proceeds through a precursor-mediated adsorption state, and the dissociative adsorption step is more facile on the gallium-rich surfaces. The ethyl and methyl ligands are thought to form Ga−alkyl species on the Ga-rich surfaces.[5−10] Methyl−Ga and methyl−As species have been proposed on the As-rich surfaces.[5,11,12] The alkyl groups leave the surface by homolysis of the carbon−metal bond to form a methyl or ethyl radical or by β-hydride elimination, in the case of ethyl ligands, to form ethylene. There is conflicting evidence for bimolecular surface coupling between alkyl ligands to form alkanes or between alkyl and hydride ligands to form alkanes. Observed alkane yields are very small relative to radical or olefin formation. Creighton and co-workers attribute alkanes to radicals reacting with chamber walls.[8,13] Murrell et al.,[14] however, argue for a direct surface reaction. This has important implications for strategies to lower carbon impurity incorporation during CVD that would use hydrogen or hydride ligands in the hope that alkanes will form because the contribution of this pathway to alkyl ligand removal is minor at best.

2.2. β-Hydride Elimination

Interest in compounds having ethyl groups as ligands was initially sparked by the lower uninten-

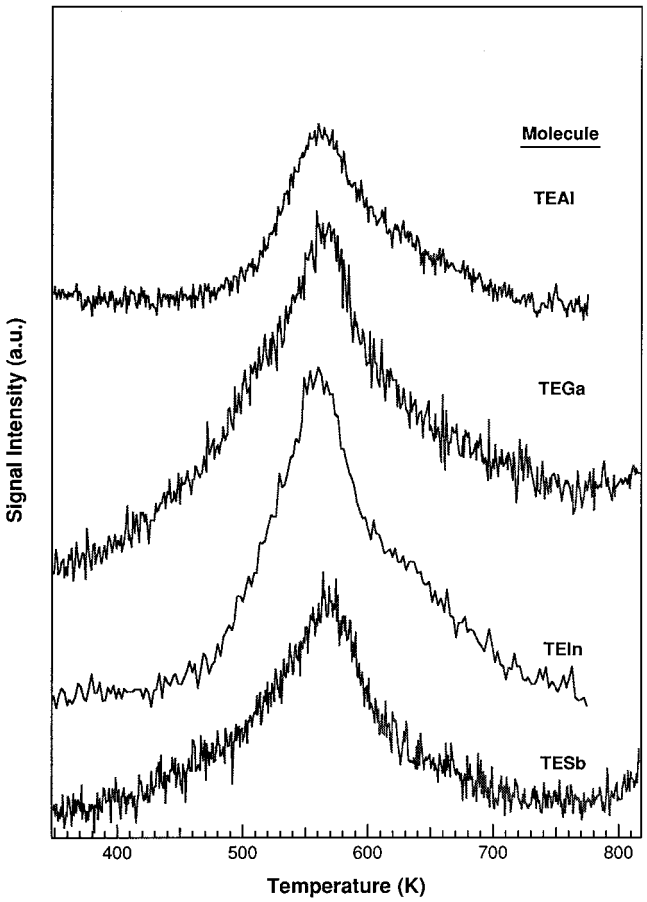

Figure 1. Thermal desorption spectra for ethylene from Ga-rich GaAs(100) following saturation exposures to triethylaluminum (TEAl), triethylgallium (TEGa), triethylindium (TEIn), and triethylantimony (TESb). From ref 10.

tional carbon incorporation during GaAs growth when triethylgallium was substituted for trimethylgallium.[15,16] Alkyl ligands in numerous organometallic compounds that feature β-hydrogens undergo facile elimination to form an olefin and a metal hydride.[17] As discussed by Elschenbroich and Salzer, a necessary condition for β-elimination is the availability of an empty valence orbital on the metal to interact with the electron pair of the $C_\beta-H$ bond. Therefore, the β-elimination mechanism plays a more important role for the organometallics of group 13 (valence configuration s^2p^1) than for those of group 15 (s^2p^3).[18] Given these guidelines, one expects the β-hydride elimination reaction to occur at the group 13 metal sites of a 13/15 compound semiconductor. Indeed the bulk of the evidence shows that alkyl elimination occurs at the Ga sites on GaAs(100).[8−10,19] It is assumed this elimination follows the β-hydride process, but still needed are isotope experiments, such as those performed on Si(100),[20] establishing that β-hydrogens are involved before we can be sure that the elimination reaction is a β-hydride process.

A recent study by Heitzinger et al.[10] showed that ethylene and hydrogen evolution from a Ga-rich GaAs(100) surface occurred at essentially the same temperature, 565 K, when triethylgallium (TEGa), triethylaluminum (TEAl), triethylindium (TEIn), and triethylantimony (TESb) dissociatively adsorbed on the surface (Figure 1). This common temperature led the authors to suggest an identical rate-limiting step for the elimination of ethyl groups from the surface following the adsorption of these molecules. Surface hydride undergoes recombinative desorption between 480 and 510 K on GaAs.[21] Since the hydride is generated during the alkyl elimination reaction above the recombinative desorption temperature, hydrogen evolves simultaneously with ethylene. This simultaneous production of ethylene and hydrogen is considered the signature of alkyl removal by β-hydride elimination.[8] Complementary SSIMS measurements show the formation of Ga−ethyl species from TESb. The ethyl groups were proposed to migrate to Ga sites and then undergo reaction at these sites during TPD. The driving force for alkyl migration from the trialkyl precursors to Ga during or following adsorption remains unresolved.

The same reactions may occur during CVD, and alkyl ligands may undergo elimination preferentially at the group 13 metal sites. However, the GaAs surface is typically As-rich during CVD, and the propensity to form group 13 alkyls from the group 13 and 15 precursors may not be the same as was observed in the surface studies. More studies will be required to resolve these questions. The reaction site is important, as precursor ligands are designed to lower carbon incorporation in CVD of compound semiconductor alloys that contain Al.

2.3. Minor Channels to Carbon

The use of trimethylgallium (TMGa) as the gallium source during epitaxial growth of GaAs often leads to high concentrations, $10^{19}-10^{21}$ cm^{-3},[22−27] of electrically active (p-type) carbon, especially when elemental arsenic sources are used, as in metalloorganic molecular beam epitaxy (MOMBE) and chemical beam epitaxy (CBE). When arsine is used, as in atomic layer epitaxy (ALE)[28−30] and metalloorganic chemical vapor deposition (MOCVD), these carbon concentrations drop to $10^{15}-10^{17}$ cm^{-3}.[1,31−33] Surface studies have proven instrumental in providing insight into arsine's role in this reaction.

Using TPD, HREELS, and SSIMS, Creighton and co-workers have identified one carbon incorporation pathway initiated by methyl group dehydrogenation and shown how dehydrogenation is suppressed in the presence of arsine.[34] In TPD, hydrogen evolves around 500 K and methyl groups desorb around 700 K, and extended TMGa exposures in the 700 K temperature regime yield substantial coverages of methylene (CH_2) adsorbate, which is detected by HREELS and SSIMS. The HREELS data (Figure 2) provide direct evidence, outlined as follows.

The well-established vibrational spectroscopy of methyl groups adsorbed on GaAs(100)[34−36] serves as a basis for comparison. To develop a substantial CH_x coverage, a Ga-rich GaAs(100) surface was exposed to TMGa (flux, 1.3×10^{12} molecules cm^{-2} s^{-1}) at 675 K for 1200 s. The surface was then flashed to 725 K to remove any residual CH_3 groups and then cooled and the HREEL spectrum recorded. The peaks at 288, 576, and 864 cm^{-1} correspond to one, two, and three phonon loss features, respectively.[34−38] This spectrum requires C−H species and is not consistent with either CH_3 or CH (the number and position of peaks are contradictory) but can be readily assigned

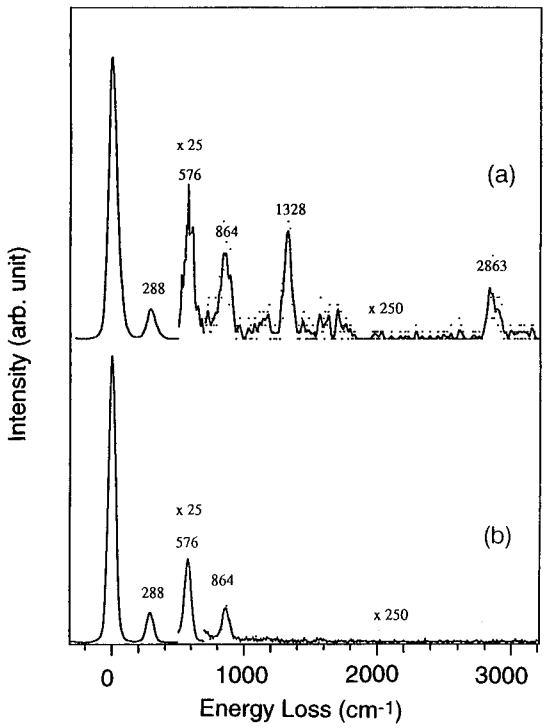

Figure 2. HREELS of Ga-rich GaAs(100) surface exposed to trimethylgallium at 675 K for 1200 s (a) and then flashed to 725 K and cooled (b). Adapted from reference 34.

to bridging (sp^3-hybridized) methylene species, CH_2. Consistent with molecular compounds, the single bending mode at 1328 cm^{-1} can be assigned to the $\delta(CH_2)$ scissors mode (in-plane bending), since it lies in the frequency range expected for such a species.[39] The 2863 cm^{-1} mode is the C−H stretching $\nu(CH_2)$, both symmetric and asymmetric.

Other features of this spectrum make minor contributions. The weak feature around 1600 cm^{-1} is consistent with a combination loss consisting of a GaAs phonon + $\delta(CH_2)$. The unresolved signal between 1000 and 1200 cm^{-1} is attributed to CH_2 wagging. Finally, there is intensity around 864 cm^{-1}, above that expected for phonons. This extra intensity could be due to a contribution from the CH_2 rocking mode, $\chi(CH_2)$.

The rate of CH_3 dehydrogenation is consistent with carbon doping levels typically obtained by MOMBE and related techniques. High-temperature exposure to arsine (AsH_3) generates surface hydride that hydrogenates the CH_2 to CH_3, which desorbs as radicals. This observation explains why carbon doping is lower during ALE (10^{18-19} cm^{-3})[28-33] than during MOMBE (10^{20} cm^{-3}).[22-27]

2.4. Nonthermal Surface Chemistry and Film Growth

For CVD and MOCVD processes, growth temperature and impurity level are important issues, especially for III−V compound semiconductors with lower congruent sublimation points, such as GaAs. Lowering the growth temperature can not only minimize contamination and interdiffusion in multilayer device structures but also reduce the process-induced defects resulting from thermal stress. The minimum temperature for epitaxial growth is determined by the precursor surface chemistry, including the adsorption kinetics, the breaking of precursor bonds, and the removal of ligands from the surface, and the surface mobility. To achieve low-temperature growth, precursor decomposition and ligand desorption must occur at lower temperature or some nonthermal method must be used to activate the film growth process. In the past decade nonthermally driven surface chemistry has attracted a great deal of attention in the surface science community.[40,41] It is now well known that photons or electrons induce bond breaking and making at the adsorbate−substrate interface. Encouraged by this discovery, researchers have widely investigated many photon- or plasma-assisted film growth technologies.[42-46] Plasma processing is widely used industrially. Photon-assisted film growth has not been adopted, but progress is promising. For example, UV irradiation enhances the deposition of metal−alkyl compounds, improving both the material quality and growth rate and allowing the deposition temperature to be decreased. It was also reported that epitaxial GaAs layers were grown in the temperature range 425−500 °C on GaAs(100) by photoassisted MOCVD using $GaMe_3$ and AsH_3.[43] Moreover, UV irradiation clearly reduces the carbon contamination originating from precursor ligands.[44] Another advantage of the photon-assisted process is the ability to deposit multilayer structures selectively on controlled areas with different thickness and doping levels.[46] Thus, making use of a focused Ar ion laser beam in conjunction with a computer-controlled X-Y scanned mirror set, multiple device structures can be accurately positioned with respect to each other on a large substrate. The low substrate temperature ensures that deposition occurs only on the areas exposed to the laser beam. This technique could generate optimum device structures without the need for selective etching of unwanted layers and selective doping by ion implantation. Reducing the number of process steps may help improve yields.

The connection between surface chemistry and film growth is very straightforward. As mentioned above, CVD or MOCVD film growth involves a number of surface chemical reactions: precursor adsorption and decomposition, ligand desorption, and surface atom rearrangement. The key questions include What role do photons or electrons play in these reactions? Do photons or electrons decompose the precursors, and to what extent? Do photons or electron remove any ligands from the surface? Do photons or electrons induce any impurity deposition by ligand decomposition? To answer these questions we cannot simply refer to gas-phase photochemistry or electron−molecule interactions because it is well known that substrates play an important role in surface chemistry. For example, substrate-quenching effect can inhibit photodissociation. On the other hand, substrate-mediated processes can provide energetic carriers to excite the adsorbates and alter product yields and distributions. To pursue the potential of nonthermal CVD technology, in recent years, photon- and electron-driven surface chemistry of film growth precursors has been widely addressed in the literature. In the following sections we review these

studies and see how some of the above questions are approached.

The photochemistry of AsH_3, the most common As source precursor, on GaAs(100) using a 193, 248, and 351 nm excimer laser[47] reveals that the initial photodissociation step is the cleavage of one As−H bond, resulting in a large fraction of H adsorbed on As sites:

$$AsH_3(a) + h\nu \rightarrow AsH_2(a) + H(a)(As)$$

AsH_2 further photodissociates to As−H and Ga−H. The final step is photochemical removal of H from Ga and As, leading to As deposition. The cross section for the first step is $\sim 4 \times 10^{-17}$ cm^{-2} at 193 nm, and it decreases with increasing wavelength. The wavelength dependence, compared to the gas-phase absorption cross section, extends to much lower photon energies, which indicates contributions from substrate-mediated excitation. Although the overall cross section for the total removal of hydrogen from GaAs(100) is relatively low ($\sim 10^{-21}$ cm^2), the high cross section for the first As−H bond cleavage by photon excitation has significance for As deposition because the dissociative adsorption coefficient of AsH_3 is very low. The photon excitation of surface AsH_3 can increase the As deposition by enhancing the effective dissociative sticking coefficient of AsH_3. Another conclusion from this study is that the wavelength selection for the photoassisted surface reaction is not so critical as in the gas phase.

More attention has been paid to Ga precursors because their alkyl ligands are the major source of carbon contamination. An early study by McCaulley et al.[48] indicates that laser-induced, pyrolytic decomposition plays a major role. They studied excimer laser-stimulated decomposition of TEGa and TMGa on GaAs surface at room temperature. Both precursors dissociatively adsorb on GaAs, whereupon irradiation by 193 nm photons leads to further decomposition and desorption of carbon-containing species. For TEGa, the decomposition rate was proportional to the laser pulse power and wavelength. At laser power above 100 mJ/cm^2/pulse, pyrolytic decomposition due to laser heating dominates and the decomposition rates are independent of irradiation wavelength. Below 100 mJ/cm^2/pulse, carbon coverage on TEGa-dosed GaAs decays at a slower rate and shows a wavelength dependence. A TMGa-dosed surface behaves similarly but with decay rates about a factor of 20 slower. Maayan et al.[49] rule out pure pyrolysis and photolysis as the only mechanisms for the photoenhanced effect they observed in the selective epitaxial growth of GaAs by photoenhanced CVD; photoexcited substrate carriers are directly involved in the photoenhanced process. Shogen et al.[50] further explore the photodissociation of trimethylgallium and trimethylindium with much lower laser power density (1−10 mJ/cm^2/pulse) on GaAs by angle-resolved photoelectron spectroscopy. For both precursors they observed metal−C bond cleavage upon 193 nm laser irradiation at 150 K. The carbon species desorb. Irradiation at 351 nm induced no photodissociation. Upon increasing the wavelength to 488 nm, pyrolytic cleavage of C−In bond occurred, and much of the generated carbon species did not desorb at 150 K. Direct detection of photodesorbed CH_3 radicals from TMGa-covered GaAs was performed by Cui et al.[51] using time of flight detection. The photodissociation cross sections were 3.1×10^{-21} cm^2 for 193 nm and 1.3×10^{-22} cm^2 for 248 nm photons.

A second chemically rich area, with potential impact for III−V compound semiconductor technologies, is growth of passivation layers on the GaAs, e.g., GaN and GaS. Unpassivated III−V compound semiconductor surfaces have a high density of midgap electronic states which adversely impact the performance of the devices. GaN and GaS reduce the number of these states. Unlike Si, oxidation of GaAs usually results in a high density of interface traps near the middle of the bandgap.

Nitrides of group 13 are, themselves, of great interest as optoelectronic materials operating at blue and ultraviolet (UV) wavelengths. Semiconductor optical devices routinely operate from the IR to green wavelengths, and recently announced extensions to blue wavelengths[52] provide a range of devices that emit and detect the three primary colors of the visible spectrum. The technological implications for imaging applications are enormous. However, progress on nitride film growth has been slowed by major difficulties in obtaining high-quality nitride-based materials. Comprehensive reviews dealing with these issues have been published.[53] For example, GaN and InN have high n-type background carrier concentrations resulting from defects commonly thought to be nitrogen vacancies. Early reports suggested that nitrogen vacancies are largely caused by the high growth temperature necessary for cracking the N-containing precursor NH_3. The best epitaxial GaN films are grown at temperatures in excess of 1000 °C.[54,55] These growth temperatures are typically used after a GaN buffer layer is grown at 500−600 °C. The latter result indicates that ammonia decomposes, at least partially, at this temperature; unfortunately, high temperatures are still required, not for initiating ammonia decomposition but for epitaxial growth.

For sulfur passivation, solutions of $(NH_4)_2S$ and Na_2S have been commonly used.[56,57] However, the chemistry is more complicated than the simple deposition of elemental sulfur. Dry deposition, e.g., with H_2S, is an attractive alternative technologically and has also been used. High temperatures are required, and the sulfide formed on GaAs is very susceptible to oxygen uptake in the presence of air.[56,57] Thus, lowering temperatures required for growth of nitrides and sulfides is a desirable goal and one which nonthermal methods can impact. There are many opportunities for chemists and engineers working together to understand how the surface chemistry of N- and S-containing precursors, activated by photons and electrons, influences film growth and the properties of model device structures, e.g., photodiodes.

The low-temperature nitridation of GaAs(100) by photon and electron irradiation of ammonia has been studied under UHV conditions.[58,59] With solid ammonia-covered GaAs(100), synchrotron radiation produces GaN, $As_{1-x}N_x$, As−H, and Ga−H species.[59] More detailed information was provided by Zhu et al.[58] where the GaAs surface was simultaneously

exposed to the UV laser and ammonia. They found that a mixture of GaN and AsN formed, with GaN dominant. With UV laser irradiation of ammonia-precovered surfaces, they found the photolysis cross section is 5.4×10^{-20} cm^2 for 193 nm photons, at a fluence $< 2 \times 10^{19}$ photons/cm^2. At fluences $> 2 \times 10^{19}$ photons/cm^2, the photolysis cross section drops, probably due to site blocking by partially decomposed and strongly bonded ammonia. The photolysis cross section decreases with increasing photon wavelength (248 and 351 nm). The reaction pathways involve both direct NH_3 excitation via photon absorption and indirect NH_3 excitation via attachment of photoexcited carriers from the substrate. For 351 nm (3.5 eV) photons, direct excitation, by comparison to gas-phase absorption, makes a negligible contribution. For this wavelength, the most likely initial excitation step would be similar to that in gas-phase dissociative electron attachment. For 193 nm (6.4 eV) photons, the direct excitation by absorption of photons may also contribute to the excitation mechanism. Using another precursor, hydrazoic acid (HN_3), Bu and Lin[60] examined photoassisted nitridation of GaAs at 120 K. At low coverage with 308 nm photons, photodissociation of HN_3 produces mainly NH_x(a), whereas at multilayer coverages, the photodissociation products include adsorbed NH_x, horizontally bound N_2, and N_3. Surface AsN and GaN were identified by TPD and XPS.

Electron-induced dissociation of ammonia has been examined by Auger electron spectroscopy (AES), TPD, and XPS.[61] Like photons, electrons induce ammonia desorption and dissociation on GaAs(100). With 50 eV unfocused electrons, the cross section for electron-induced desorption and dissociation is 1 order of magnitude higher than that for photons. With a focused electron beam from an Auger electron gun, a nitride film was formed by simultaneously exposing the GaAs surface to ammonia and the electron beam. The effect of beam energy on the nitridation rate is not significant over the range between 350 and 3000 eV. This implies that core level excitation of N is not dominant, since 350 eV lies below the threshold. More likely, low-energy secondary electrons, generated by the incident beam, resonantly produce, temporarily, anionic forms of ammonia which live long enough to dissociate.

Photoassisted sulfur deposition has been examined using two S-containing precursors, H_2S and elemental S.[62−64] Both form sulfides under photon irradiation. On GaAs(100) c(8×2), Nooney et al.[62] found that, without photon assistance, only one monolayer of S could be built up by repeated cycles of H_2S exposure at low temperature followed by heating to 600 K. When 193 nm photons were used, thicker and unsaturable sulfide layers were produced. Auger studies indicate that As remains below the GaS_x layer up to 600 K. The authors propose that GaS and GaS_2 are both involved. However, on a different surface, GaAs(001), mainly AsS was formed after ArF excimer laser irradiation in an H_2S ambient.[63] This may related to the GaAs surface structure, as well as the surface temperature. For example, GaAs(100) c(2×8) is a Ga-rich surface, which may favor GaS rather than AsS. This is indicative of the interesting chemical structural and reactivity issues that remain unresolved.

Elemental S, which exists in gas phase as an S_8 ring, is an alternative sulfiding source. Compared to H_2S, elemental S does not have the potential problem of hydrogen penetration into surface, an undesirable effect since it passivates bulk donors and/or acceptors. UV light irradiation dissociates S−S bonds and S deposits onto GaAs.[64] Photoluminescence, which can measure optically active defects, indicates that the passivation layer is of at least the quality produced by conventional $(NH_4)_2S$ solution treatment. Interestingly, this study makes the point that surface oxygen is not replaced by sulfur, so that optimizing passivation requires the removal of native oxide.

Another interesting study,[65] related to nitridation but not of GaAs, shows how nonthermal events can play a major role in the ligand removal that controls the film growth rate. For the reaction of Si(100) with NH_3 at 90 K, they found no significant activation barrier for dissociative adsorption of ammonia. Even at this low temperature, the surface dangling bonds readily dissociate NH_3 to N and H atoms. When N atoms occupy subsurface sites, H atoms bind to Si surface dangling bonds and passivate the surface for further dissociative adsorption. Thus, to sustain film growth thermally, elevated temperatures are critical; hydrogen must be removed to regenerate the surface dangling bonds. Bozos and Avouris[65] showed that silicon nitride film growth can be sustained, even at 90 K, provided the surface hydrogen is continuously removed by electron-stimulated desorption, Figure 3. Without electron irradiation during ammonia exposure, the N(KLL) Auger peak intensity reaches no more than 14% of the intensity of the Si(LVV) peak, and the latter remains characteristic of unreacted elemental Si. When the surface is simultaneously exposed to NH_3 and 1.2 keV electrons, the N(KLL) signal increases about 10-fold. Meanwhile, the unreacted Si(LVV) signal is eliminated and replaced by a signal characteristic of silicon nitride. Further evidence for a nitride film is provided by electron energy loss spectroscopy; the elemental Si surface and bulk plasmon excitation features were replaced by a broad plasmon loss at 21 eV, characteristic of Si_3N_4. The thickness of the nitride film grown at 90 K with the help of electron irradiation is about 20 Å. The major role of the electron irradiation is to maintain a hydrogen-free Si surface which actively dissociates NH_3.

2.5. Summary

To summarize, surface chemistry studies, linked to compound semiconductor film growth, are providing critical, fundamental information which can be used to evaluate the technological potential of nonthermal activation processes. Synthesizing novel precursors with reactivity and stoichiometric properties desired by film growers is a challenging avenue for research. Building on a rich and diverse base of molecular knowledge, the kinetic characterization of the surface chemistry of conventional and novel precursors is providing fundamental data that can potentially be used in engineering modeling of film

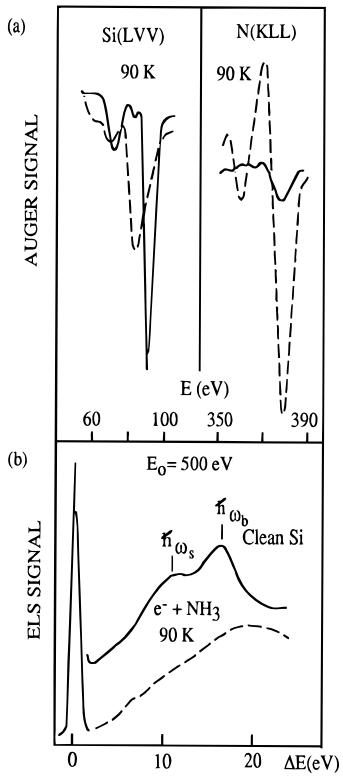

Figure 3. (a) Si(LVV) and N(KLL) Auger spectra of Si(100) surface after exposure to 900 s at 10^{-7} Torr of NH_3 at 90 K (solid lines) and after simultaneous exposure to the same NH_3 dose and 30 μA, 1200 eV electron beam at 90 K (dashed lines). Area of surface exposed to the electron beam: ~4 mm^2. (b) Electron energy loss spectra of the clean Si(100) (2×1) surface (solid line) and the surface produced by simultaneous exposure to NH_3 and the electron beam as in part a (dashed line). From ref 65.

growth reactor systems. As other examples set forth here indicate, there are many cases where photons and electrons do activate nonthermal channels for precursor decomposition chemistry. Since photon and electrons are expensive, compared to thermal energy, the extent to which they can be used fruitfully in commercial manufacturing remains to be determined. As illustrated by AsH_3 on GaAs, after the first bond cleavage, the fragments often bond to the substrate more strongly than the precursors, and often, the competitiveness of substrate quenching increases, making further nonthermal bond cleavage less probable. Nevertheless, efficient cleavage of the first bond is desirable because it greatly increases the dissociative sticking coefficient and, thereby, potentially, the film growth rate when this step limits the rate of mass accumulation. Thus, we are lead to consider nonthermal activation coupled to thermal pulses as a plausible manufacturing strategy—nonthermal to enhance cleavage of the first bond and thermal pulses to drive further decomposition. The photon-activated chemistry described here reveals that the wavelength response for surface reactions is generally much less structured, i.e., effectively nonresonant, compared to the gas phase. This is ascribed to a major role for substrate-mediated processes; electronic excitations in the substrate are followed by numerous scattering events which lead to hot carriers distributed broadly in energy. Thus, we expect that wavelength selectivity, a powerful tool for manipulating gas-phase photochemistry, will be diminished for photon-driven surface chemistry. These investigations of photon- and electron-initiated chemistry at surfaces illustrate concepts and provide potentially useful guidelines for designing and improving film growth technologies.

3. Silicon-Based Semiconductors

As noted earlier, the silicon-based technologies account for by far the largest fraction of electronic materials business worldwide. Advances in these technologies often involve incremental improvements which, when multiplied by the business volume involved, can have enormous economic impacts. In this enterprise, there are many chemical questions regarding structure and kinetics begging for answers. This section introduces and overviews a cross section of steps used in silicon-based device processing, including semiconductor film growth, dielectric film growth and modification, metalization for electrical contacts and barrier materials, and etching. We also discuss interface issues that are probed by optical spectroscopy. Since these topics do not involve the common theme of precursor adsorption and decomposition that was used in the discussion of 13−15 compound semiconductors, each section presents pertinent background material and a discussion of the technological issues that the surface chemistry studies address.

3.1. Si–Ge Hydride Chemistry

Future silicon-based electronic devices may well involve alloys of silicon with germanium and carbon. For example, heteroepitaxial growth of pseudomorphic $Si_{1-x}Ge_x$ on Si(100) is receiving considerable attention because of the bandgap engineering possibilities afforded by alloys.[66] Heterojunction bipolar transistor devices have been demonstrated with pseudomorphic layers; these alloys should permit silicon-based devices to operate at lower power and voltage. Among the key problems involving chemical issues are control of film thickness and composition. For example, the strong dependence on Ge surface concentration of precursor decomposition rates and, as a result, the film growth rate leads to problems in controlling the properties of these alloys.[67] Thus, understanding and manipulating the surface chemistry of the precursors and surface hydrides are central to growth of device quality films.

Hydrides are among the most widely used precursors, and their adsorption and kinetic behavior (SiH_4, GeH_4, Si_2H_6, and Ge_2H_6) have been reported over Si(100) and Ge(100) surfaces.[68−72] Modeling studies have shown that at high temperatures or low flux rates, the dissociative adsorption processes control the rate, and at lower temperatures and high flux rates the hydrogen desorption is rate controlling.[67,73−76] Regardless of the growth temperature, hydrogen desorption puts a maximum limit on the growth rate; conversely, hydrogen desorption places a minimum on the temperature for a desired growth rate, and thus, desorption of hydrogen from $Si_{1-x}Ge_x$ surfaces is a central issue.

Although there is general consensus regarding the surface processes and reactions on Si(100) and

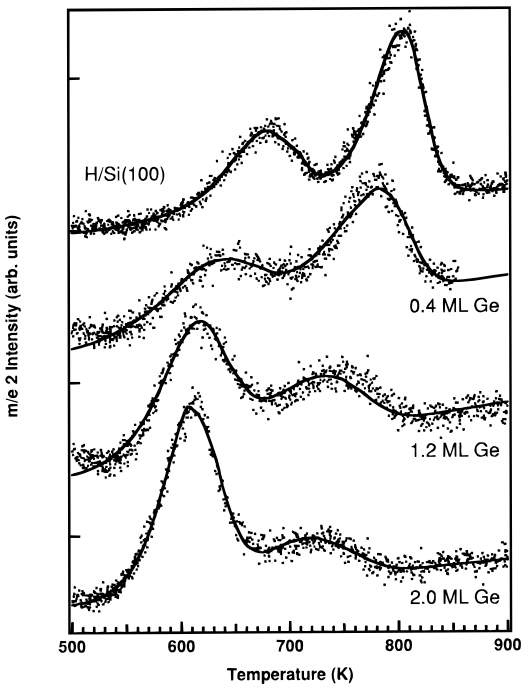

Figure 4. H_2 TPD from Si(100) and Ge-covered Si(100) following saturation exposure to atomic H at 400 K. The heating rate was 5 K/s. One monolayer of Ge is equal to 6.78×10^{14} cm^{-2}. From N. M. Russell, unpublished work.

Ge(100) surfaces, hydride reactions on alloy, $Si_{1-x}Ge_x$, surfaces are less well understood. There are two hydrogen desorption states from Si(100), a monohydride β_1-state and the dihydride β_2-state. Figure 4 (top curve) presents typical TPD spectra for H_2 desorption from Si(100). The mechanism for H_2 desorption has been discussed in several publications;[71,72,77,78] the key features are desorption from the dihydride and monohydride states, surface reconstruction from 1×1 to 2×1 during which the dihydride converts to a monohydride, and pairing of the monohydride sites with dimer vacancies. Hydrogen desorption from Ge(100) proceeds exclusively from a monohydride state (termed the α-state), and as with Si(100), pairing of monohydride dimers and vacant dimers is expected. A TPD profile from a Ge-rich surface is shown in the bottom curve of Figure 4.

The activation energy for desorption from Si(100) is considerably higher ($\beta_1 = 56$ kcal/mol and $\beta_2 = 42$ kcal/mol) than from Ge(100) ($\alpha = 34$ kcal/mol). This difference in activation energies leads to increases in the growth rate as the Ge surface concentration increases because more of the surface hydride, which blocks dissociative adsorption of the gaseous Si and Ge precursors, can desorb from the surface.[79−81] This has been referred to (incorrectly) as the catalytic effect of Ge on the film growth. The TPD profile for desorption from Si(100) with differing amounts of surface Ge, Figure 4, is consistent with data reported by Crowell and co-workers.[68−70] Crowell has associated this shift in desorption with parallel desorption from both Si monohydride and Ge monohydride but with the activation energy for desorption from Si sites lowered by an electronic effect. Considerably less electronic effect is needed if a Si monohydride/Ge monohydride exchange reaction is included.[82] We add the additional step in which Si monohydride exchanges with Ge dimer vacancies to form a Ge monohydride dimer. (The reverse step, germanium monohydride to silicon monohydride, has been demonstrated and discussed.[70]) The predicted mechanism for this exchange and the resulting energy diagram are presented in Figure 5. By forcing the reactions at Si and Ge sites to be those found for Si(100) and Ge(100) surfaces, respectively, we are able to fit TPD data for varying Ge coverage (solid lines in Figure 4) and predict an activation energy for migration from Si to Ge of 24 kcal/mol.

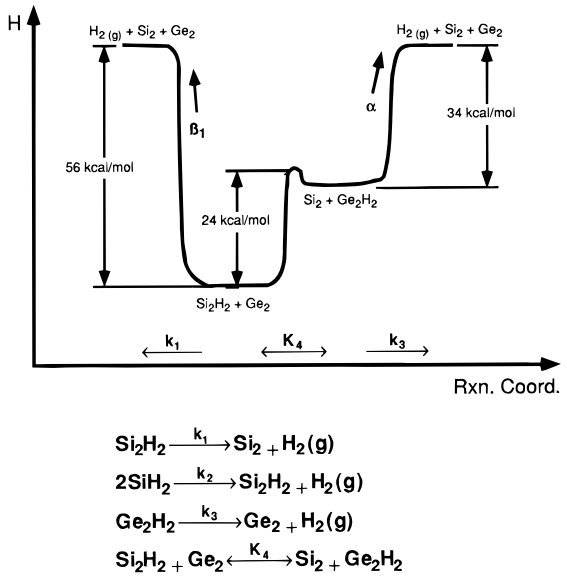

$$Si_2H_2 \xrightarrow{k_1} Si_2 + H_2(g)$$
$$2SiH_2 \xrightarrow{k_2} Si_2H_2 + H_2(g)$$
$$Ge_2H_2 \xrightarrow{k_3} Ge_2 + H_2(g)$$
$$Si_2H_2 + Ge_2 \xleftrightarrow{K_4} Si_2 + Ge_2H_2$$

Figure 5. Simple reaction scheme for hydrogen desorption from $Si_{1-x}Ge_x$ surfaces and a reaction coordinate diagram illustrating the energy between the surface states. From N. M. Russell, unpublished work.

In addition to the insights gained from TPD experiments, second-harmonic generation (SHG)[83−103] is an emerging technique to probe the kinetics of Si−Ge film growth and hydrogen desorption. SHG can operate in all pressure regimes, provide real-time signals,[98,101,103] penetrate transparent films to probe buried interfaces,[88−90] and nondestructively characterize various surface properties of the material.[91−100] Studies are now underway to uncouple the role of interface characteristics (strain), surface space charge, and bulklike effects on the nonlinear polarization response of silicon alloy surfaces. These will form the basis for establishing SHG as a quantitative probe of the surface chemistry. Below we give two examples that demonstrate the potential to probe *in-situ* Si film growth with SHG.

One of the first experiments using optical SHG to study the deposition of Si and Ge on silicon was performed by Hollering et al.[98] In that work, the real-time deposition of Si and Ge atoms on Si(001)-2×1 was correlated to the SH signal intensity. At room temperature the initial deposition of Si caused the SH intensity to decrease rapidly, indicating the disruption of long range surface order. In contrast, when the substrate was held at 750 K, the SH signal remained constant. This behavior of the SH signal at elevated temperature was also observed by Heinz et al.[101] in 1987 and serves as a signature of epitaxial growth conditions. For Ge deposition at room temperature, the SH signal reached a maximum at 1 ML and subsequently decayed to a constant level by 3

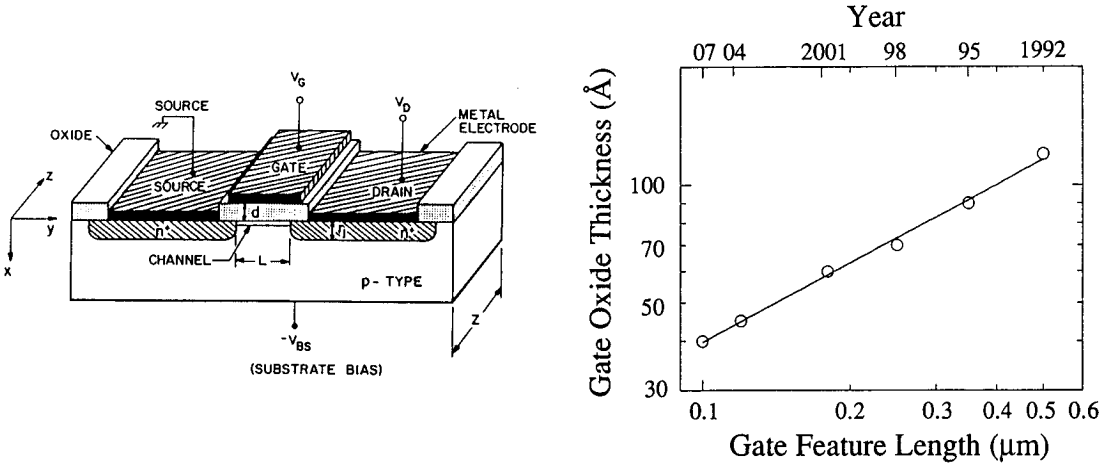

Figure 6. Diagram of MOS gate structure (left) and gate oxide thickness vs gate feature length (right). From D.-L. Kwong, unpublished work.

ML. These results correlate well with the known mechanism of Ge epitaxial growth on Si.[102] At 1 ML the maximum number of Si−Ge bonds is obtained and corresponds to the observed maximum in the SH signal. Above 1 ML, the Si−Ge interface is buried as two-dimensional layer-by-layer growth of Ge proceeds, resulting in the measured decrease of the SH intensity. These results demonstrate the unique ability of SHG to provide real-time evaluation of a growing film.

Recently Dadap et al.[103] have exploited femtosecond SHG to monitor Si epitaxy under CVD and ALE growth conditions with unprecedented data acquisition speed and efficiency. In the CVD growth mode, silicon was deposited from disilane onto a 20 Å $Si_{0.9}Ge_{0.1}$ film on a Si(100) substrate heated to 925 K. Immediately after the disilane (4% in He) was introduced into the chamber at a pressure of 5×10^{-4} Torr, the time dependent SH intensity was recorded. The SH signal displayed a damped oscillation for a few hundred seconds, eventually reaching a constant level after ~1000 s. This behavior was attributed to the interference between scattered light at the growing Si layer and $Si_{0.9}Ge_{0.1}$ interface, ceasing when the Si layer thickness exceeded the penetration depth of the laser light. Also, in experiments designed to probe several key stages of the self-limiting growth of Si on Si(100), Dadap et al. used SHG to follow the adsorption and desorption of hydrogen. While dosing disilane at 425 K, the SH signal tracked the uptake of the monohydride and dihydride adsorption states of hydrogen. This should enable sticking coefficients for hydride precursors to be measured as a function of surface coverage and in the presence of coadsorbates. Subsequently, the temperature of the dosed surface was ramped at 1 K/s from 425 to 875 K while recording the SHG response. The signal dropped around 627 and 737 K and was associated with the onset of the dihydride and monohydride desorption peaks, respectively, that are observed at comparable temperatures during separate TPD experiments.

In short, these SHG experiments illustrate the *in-situ* ability to characterize the thickness, growth rate, and adsorption−desorption kinetics of the technologically important interface of $Si_{1-x}Ge_x$. When these studies are coupled to macroscopic reactor models, one should be able to predict the effects of flux, temperature, and gas composition on growth rates and film composition and thereby control the processing of $Si_{1-x}Ge_x$ films to the tolerances needed in device applications.

3.2. Oxynitride Film Growth

A primary goal of microelectronics manufacturing is to pack more and more features, e.g., transistors, into a smaller and smaller area or volume, thus increasing the speed and information density in a given ULSI device. Each transistor contains a gate dielectric to switch a transistor's current on and off (Figure 6). As the size, width, and height of circuit features continue to decrease into the submicron regime (a human hair has a diameter of ~10 μm), new materials problems emerge, especially under conditions where the width or height length scale becomes only a few times the crystal lattice parameter of the materials in question. For example, a present engineering goal is to reduce feature lengths in gate dielectrics to 0.18 μm and scale the thickness down to at least 6 nm, and preferably lower. To realize a gate length of 0.1 μm, the thickness goal drops to 4 nm. These thicknesses are of order 10 unit cell lengths, with interfaces to different materials above and below. In general, at an interface between two solid materials, a few unit cell lengths are required to pass from the bulk properties of one material to the other, e.g., doped Si to SiO_2. In pursuing the manufacturing goals for thin dielectrics, the interface regions become a large fraction of the total, and their properties can dominate. Manipulating the chemistry that accompanies the formation of these interfaces is of great importance in determining their final structural and electronic properties which, of course, have a direct bearing on the electrical properties.

Conventionally, thermal silicon dioxide (SiO_2) has been used as the gate dielectric in MOS devices. Because they are strained, the oxygen−silicon bonds in the interface region are vulnerable to damage by energetic charge carriers that are injected during operation.[104,105] Thus, defects are generated, and when the interface dominates the electrical properties, such defect generation shortens the lifetime to unacceptable values. SHG has been used to probe

for these defects and other interfacial properties.[88−90,106−110] While the nonlinear response of the SHG signal is complicated and better theoretical understanding of the excitations occurring at the SiO_2/Si(100) interface is needed, SHG has enormous potential. An illustrative example is seen in the work of Dadap et al.[111] who utilized SHG to characterize the interfacial roughness of SiO_2/Si{100}. The roughness was systematically varied by changing the duration of a 7:1 NH_4F:HF-buffered oxide etch. The hydrogen-terminated surfaces were then imaged in air with an atomic force microscope to quantitatively determine the root-mean-squared roughness values. After a native oxide layer was grown, polarization dependent SHG measurements were taken. The results are displayed in Figure 8. In the top row, two trends are evident in panels a−c: Both the amplitude of the p−p (p-polarized fundamental, p-polarized second harmonic) oscillation and the offset decrease as the roughness increases. In contrast, the middle row of panels shows no variation for p−s configuration (p-polarized fundamental, s-polarized second harmonic). In accordance with theory,[87] these two results demonstrate that the p-polarized second-harmonic light is sensitive to interface roughness, while s-polarized light from the bulk is unchanged by the physical state of the interface. These results suggest that SHG can serve as a rapid, noninvasive method to ascertain angstrom scale roughness.

To improve the performance of devices involving thin SiO_2 layers, oxynitrides of silicon are being investigated.[112−129] In addition to reducing hot carrier damage, oxynitrides limit dopant diffusion, e.g., B, from Si into the oxide and, thus, are a superior barrier material at interfaces of thin SiO_2 with silicon.[130,131] From the perspective of Figure 6, it would be desirable to have N incorporation into the silicon oxide at both the channel−gate and gate−gate oxide interfaces. This would provide a barrier to B diffusion at both and remedy the problem of oxide reliability and invasion of the substrate by diffusing B. Keeping B out of the gate oxide region is helpful because its presence there tends to degrade the electrical properties, in particular, the transconductance, g_m, of the device structure, i.e., the ability of the gate voltage to control the current through the device. It is desirable to have the current drop or increase very sharply with changes in the gate voltage:

$$g_m = \frac{i_d}{V_g}$$

where i_d is the drain current and V_g is the gate voltage. Boron in the gate oxide regime tends to drive down g_m, weakening the control.

Currently, a widely used multistep procedure involves N_2O oxidation and NH_3 nitridation followed by O_2 reoxidation of the nitrided oxide (ROXNOX). These engineering steps, while realizing improved reliability, are based on empirical knowledge rather than on strong physical−chemical foundations. Elucidation of the chemical nature of the interfaces formed during these processes would be enormously helpful to engineers now searching for more economical and effective routes to these dielectrics. Nitrous oxide oxidation at atmospheric pressure forms an interfacial dielectric that resists hot carrier damage but does not meet B diffusion barrier requirements, presumably because of limited N incorporation. The latter is improved by NH_3 nitridation because a N-rich layer is formed, but residual H leads to deterioration of electronic properties by incorporating electron traps. Thus, O_2 reoxidation is used to reduce the residual H content but leaves some undesirable electrical properties. While NH_3-nitrided SiO_2 may have relatively high amounts of nitrogen in the film (1−5 atom %), N_2O-grown oxides typically have much lower levels.[132,133] While the combination of steps described above has benefits, they are clearly limited.

From a surface chemical perspective, N_2O oxidation followed by NH_3 nitridation might be replaced by NO_2 oxidation. NO_2 is very corrosive compared to N_2O, and by suitable choice of operating conditions, it might be possible to increase the atomic N concentration by delivering this molecule containing a very active nitrogen atom. Recently, an ultrahigh vacuum surface chemistry study showed that the nitridation of clean Si(100)-2×1 with NO_2 leads to the efficient incorporation of nitrogen (N) and oxygen (O) compared to N_2O.[134] While comparison with N_2O at this ultrahigh vacuum dosing level does not connect directly to conditions of atmospheric oxidation and nitridation, the inference is clear.

At 800 °C, as little as 10 langmuirs of NO_2 gives detectable O and N AES signals; for N_2O, there is no detectable signal even after an exposure of 800 langmuir at 800 °C. Figure 7 shows, for selected doses (10, 100, and 300 langmuir) of NO_2, how the AES atomic ratios vary with temperature between 25 and 1000 °C. The N/Si ratio, Figure 7a, increases slowly at temperatures below 500 °C, independent of exposure. At higher temperatures N/Si, in agreement with ref 135, increases sharply with exposure. The N/O ratio follows a similar pattern, Figure 7b. The likely reason for this behavior is diffusion-limited incorporation of N and O, much like the NO/Si system.[136] NO_2 incorporation is likely to proceed via a two-step process: (i) initial passivation of dangling bonds with N and O and (ii) further slow diffusion of N and O. The decay of O/Si, Figure 7c, is expected since oxides decompose, desorbing SiO and leaving sites for more incorporation of N. Nitride decomposes, ejecting Si_2N, at much higher temperatures, 1075 °C.[137]

The incorporation of N and O through a nitrogen-rich layer has been studied by repeated dosing (NO_2 at 700 °C) and annealing (900 °C) cycles. The N/Si level continues to grow, while the O/Si level remains nearly constant. This finding could be interpreted in two as yet unresolvable ways: (i) At 700 °C, N diffuses to subsurface sites, leaving surface dangling bonds available for subsequent O incorporation, or (ii) on the basis of Rangelov's model,[136] N and O diffuse into the substrate after the formation of an initial passivation layer that does not inhibit subsequent N and O diffusion. The accumulation of N, despite the presence of a pre-existing nitrogen-rich layer, points to one way of surmounting the difficulties associated with N_2O and NH_3 processing.

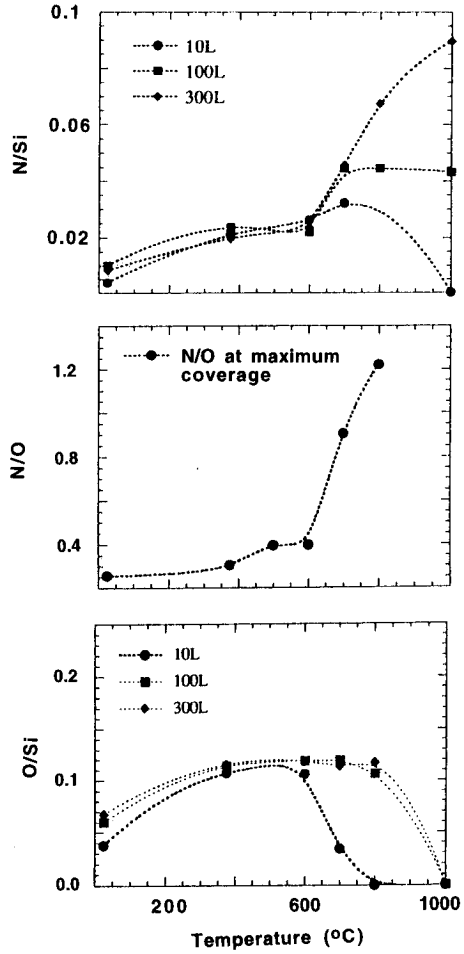

Figure 7. Summary of (a) N/Si for clean Si surface exposed to 10, 100, and 300 langmuir of NO_2, (b) N/O for clean Si surface exposed to 500 langmuir of NO_2, and (c) O/Si for clean Si surface exposed to 10, 100, and 300 langmuir of NO_2 at varying substrate temperatures. From ref 134.

As noted above, it is not possible to compare UHV directly with atmospheric pressure processing, i.e., furnaces or rapid-thermal-process (RTP) systems. It is important to bear in mind that the temperature required in an UHV system to obtain a given concentration of N or O is higher than that required in a semiconductor process chamber. By mass action, higher operating pressures aid the incorporation of N and O. For example, the reaction of Si with N_2O yields no N or O chemisorption under UHV, whereas in a furnace or RTP system a small amount of N (~1%) is incorporated.[114] Building on the simple mass action concept, recent evidence suggests that N_2O oxidation at ~25 atm leads to significantly higher levels of N incorporation into gate oxides and that the temperature can be reduced from 1000 to below 850 °C. Angle-resolved XPS analysis (ARXPS) focusing on the N(1s) region indicates that the incorporated N is in the near-surface region. ARXPS was accomplished by tilting the sample with respect to the analyzer direction, changing the effective sampling depth from 21 to 75 Å. Before sputtering, the N(1s) signal rises as the sampling depth is decreased, while the substrate Si peak decays and the oxide Si peak grows. After removal of 20 Å by sputtering, the N(1s) signal is absent, while the substrate Si peak is stronger but still decreases (the oxide peak grows) as the sampling depth decreases. This result is encouraging, since there is enough N at the upper surface to serve as a barrier layer against B diffusion from a poly-Si gate subsequently placed over it.

3.3. Copper and Titanium Nitride Deposition

The deposition of metals and barrier layers are two other microelectronics areas in which surface chemical science and technology interact closely. These materials, and the interfaces between them, are of central importance for wiring together the active components of multilevel integrated circuits. Deposition can be realized by physical vapor deposition (PVD) processes that employ evaporation and sputtering of elemental sources. Since the 1960s, CVD using molecular precursors has been increasingly studied for deposition on integrated circuits. While PVD works well to deposit material on surfaces in line-of-sight of the source, conformal deposition of rough surfaces is a crucial issue. This issue becomes very critical for integrated circuits with feature sizes less than 0.5 μm because trenches with rather high aspect ratio (height to width) must be coated uniformly (conformally) and/or filled.[139]

Compared to PVD, CVD processes are more complex because, by their very nature, chemical reaction mechanisms are involved. For CVD metal deposition, an often large and complex metal precursor is delivered onto a substrate held at a fixed temperature, and then the precursor decomposes and deposits metal on the surface. This requires that the metal−ligand bonds be readily cleaved, while the ligands must not decompose on the surface but rather desorb, directly or indirectly, so that only metal atoms are incorporated into the film. For nitride CVD, it is usual to employ separate precursors for the metal and the nitrogen.

We focus on Cu and TiN deposition, an area of rapid growth over the past few years.[140,141] Cu is proposed as a possible replacement for aluminum for the metalization of ULSI circuits. Al and its alloys have been commonly used as metalization materials, and they meet many of the requirements for conductors in large scale integrated circuit structures. However, Al suffers major limitations from its resistivity, which is higher than for copper, and from electromigration in submicron devices. The electrical resistivity of Cu is 1.7 $\mu\Omega$ cm, versus 2.7 $\mu\Omega$ cm for Al. In addition, Cu has superior electromigration reliability, about 2 orders of magnitude higher than that of Al.[142] However, Cu does present some problems. First, Cu tends to diffuse rapidly through typical adjacent materials. Second, Cu surfaces are difficult to passivate, which makes interfaces vulnerable to corrosion, jeopardizing their electrical integrity. Therefore, the integration of copper metalization with SiO_2 or other insulators with lower dielectric constants introduces a number of interesting problems, many of which involve solid state chemistry at interfaces.[143] To prevent surface oxidation and inhibit interdiffusion of Cu into substrates, a variety of barrier layer compounds has been tested.[139,144,145] TiN is very promising for this purpose because of its low resistivity (~22 $\mu\Omega$ cm) and excellent barrier properties[140,146,147] and because it is currently used

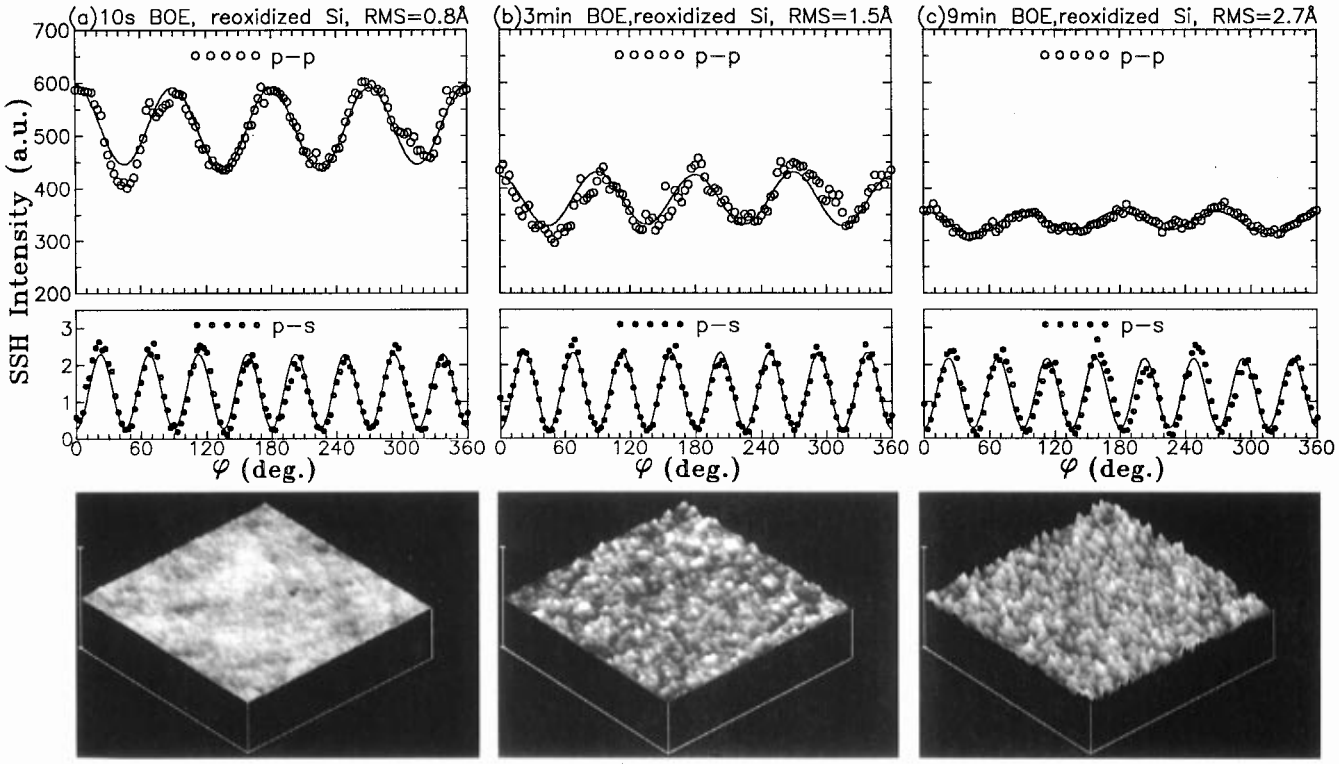

Figure 8. Surface second-harmonic intensity vs φ in reoxidized Si(100), p−p configuration (open circles, top panel) and p−s configuration (filled circles, middle panel), for (a) 10 s, (b) 3 min, and (c) 9 min buffered oxide etch (BOE) exposure. The solid lines are the corresponding fits to the data. The corresponding AFM scans in the bottom panels show the rms values of 0.9, 1.5, and 2.7 Å, respectively. From ref 111.

in some Al metalization systems; thus, there is a body of experience and equipment already accumulated. Although the most effective technique for depositing TiN is reactive sputtering, this technique has drawbacks for ULSI fabrication. Thus, development of a CVD process for TiN has been of increasing interest, and there are examples of high-quality TiN films grown at low temperatures by CVD.

An important issue in Cu CVD is the selectivity. For microelectronics device applications, we need either selective deposition or selective etching to form patterned copper wires. Deposition selectivity depends on the substrate materials; e.g., deposition might occur readily on metal but not the insulator surfaces. Because of the absence of a viable anisotropic dry etching process for Cu, selective deposition appears to be an important alternative. The factors affecting the selectivity and the underlying mechanisms have been addressed by surface science studies, in which a variety of Cu precursors has been synthesized and tested.[148,149] In general, these precursors can be divided into two groups, differentiated by the Cu oxidation state (2+, designated II, or 1+, designated I) in the precursor. Among these precursors, the copper(I) and copper(II) diketonate complexes have shown the best results. High-quality copper with conformal filling of submicron features has been achieved. The chemical structures and acronyms of these complexes are listed in Table 1. Further comparison shows that the Cu(II) group precursors have high thermal stability and high vapor pressure, which ease the delivery of the compound to the deposition chamber.[150] The deposition rate, however, is relatively low, and high substrate temperatures are required. In addition, the presence of a reducing agent, such as hydrogen, is necessary for the surface reaction. In contrast, the conversion efficiency of Cu(I) group precursors to copper films is quite high, although the vapor pressure of Cu(I) precursors is fairly low. The CVD process with Cu(I) precursors requires no reducing agents. The disproportionation reaction relies on electron donation in order to proceed, implying that Cu(I) precursors can inherently selectively deposit copper onto a conducting surface. For these reasons, the current Cu CVD research focuses on the copper(I)β-diketonate. These precursors have the formula (β-diketonate)CuL, where L is a neutral ligand and

Table 1

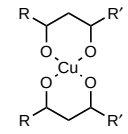

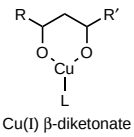

ligand	abbreviation
acetylacetone, R = R′ = CH_3	acac
1,1,1-trifluoro-2,4-pentanedione, R = CH_3, R′ = CF_3	tfac
1,1,1,5,5,5-hexafluoro-2,4-pentanedione, R = R′ = CF_3	hfac
1,1,1,5,5,6,6,7,7,7-decafluoro-2,4-heptanedione, R = CF_3, R′ = C_3F_7	dfhd
1,1,1,2,2,3,3,7,7,8,8,9,9,9-tetradecafluoro-4,6-nonanedione, R = R′ = C_3F_7	tdf
L = vinyltrimethylsilane	VTMS
L = bis(trimethylsilyl)acetylene	BTMSA
L = 1,5-cyclooctadiene	COD
L = 1,5-dimethyl-1,5-cyclooctadiene	1,5 DMCOD
L = 1,6-dimethyl-1,5-cyclooctadiene	1,6-DMCOD
L = dimethyl-1,5-cyclooctadiene	DMCOD

β-diketonate is hexafluoroacetonate (hfac). The deposition occurs via the following facile disproportionation reaction:[127]

$$2(\beta\text{-diketonate})CuL \rightarrow Cu(s) + Cu(\beta\text{-diketonate})_2(g) + 2L(g)$$

The mechanism of selective deposition has been extensively studied from the surface science point of view.[151−157] The first step in the deposition process is the chemisorption of precursors onto the surface. Depending on the substrate, the precursor dissociates into RCu and L species or desorbs intact from the surface. For selectivity, both are desired. In dissociative adsorption, L is usually more volatile and quickly desorbs, leaving RCu species on the surface. Next, the two RCu species react to form Cu metal and Cu(II) species, R_2Cu, the latter volatile and easily desorbed from the surface.

According to this mechanism, once the precursor has chemisorbed, there are two competing reactions: intact desorption and dissociation into L and RCu. This competition is largely determined by the relative strengths of the chemisorption bond and the Cu−L bond. In order to suppress the deposition of Cu on, for example, SiO_2 and promote deposition only on the metallic surface, it is important to identify the SiO_2 chemisorption sites. The active chemisorption sites for Cu(I) precursors are the hydroxyl groups,[150,151] which may be either isolated or hydrogen bonded together. Using transmission Fourier transform infrared spectroscopy (FTIR), Dubois and Zegarski[152] found that on clean SiO_2, (hfac)Cu(VTMS) desorbs intact below room temperature with no Cu deposition. However, the selectivity was lost if the surface was exposed to water or ethanol to produce adsorbed hydroxyl groups before the adsorption of the precursor. They found that the selectivity could be lost in other ways as well: too hot a precursor, too high a substrate temperature, or the presence of adsorbed metal centers. Clearly, intact desorption is the key issue for selective deposition. Strengthening the chemisorption of precursors, or promoting dissociation, either by predissociating the precursor in the gas phase or by raising the substrate temperature, causes a loss of the selectivity. Therefore, if the surface hydroxyl group is removed or passivated, the selectivity can be recovered.[150−152]

The bond strength between L and Cu has been investigated through thermal desorption studies on Cu(100).[152] The desorption temperatures of ligands from Cu quantitatively represent the bond strength between ligands and Cu. Results are, for 2-butyne, a desorption temperature of 130 K; for VTMS, 180 K; for 1,5-COD, 220 K; and for PMe_3, 430 K. The trend of the bond strength is very consistent with results of the selectivity studies for precursors with these ligands.[153−156] A precursor with L = 2-butyne shows no selective deposition, while very selective deposition occurs on metals over SiO_2 when L is replaced by $(P(CH_3)_3)(PMe_3)$. The compounds containing L = 1,5-cyclooctadiene (COD) and vinyltrimethylsilane (VTMS) show intermediate selectivity. The weaker the Cu−L bond, the less selective the precursor. In summary, weaker chemisorption and stronger Cu−L bonds favor selective deposition.

Although CVD growth of a TiN layer has been realized using $TiCl_4$ and ammonia as precursors,[137,158] the growth temperature of ~600 °C is too high for TiN deposition in the presence of aluminum. Recently, tetrakis(dimethylamido)titanium ($Ti(NMe_2)_4$) and ammonia have been used to deposit high-quality TiN films[159] at ~300 °C. A stoichiometric reaction between the two compounds is

$$6Ti(NMe_2)_4 + NH_3 \rightarrow 6TiN + 24NHMe_2 + N_2$$

Surface adsorption studies show that $Ti(NMe_2)_4$ adsorbs on $TiSi_2$, Al(100), and Cu(100) with an initial sticking coefficient near unity at 300 K. Heating the $Ti(NMe_2)_4$-precovered $TiSi_2$ and Al(100) leads to the decomposition of $Ti(NMe_2)_4$ and yields films containing Ti, N, and C. On Cu(100), however, there was no thermal decomposition below 400 K. Under UHV conditions, there is no interaction between $Ti(NMe_2)_4$ and ammonia on these surfaces at temperatures between 300 and 650 K. This is in sharp contrast to what is observed in the gas phase, where the reaction proceeds rapidly and produces dimethylamine. Here, a gas-phase reaction is believed to be as important as the surface chemistry: the intermediate in the gas-phase reaction may be responsible for the surface reactions that result in the growth of the TiN film. The deposition mechanism was further studied by using isotopic substitution with $^{15}NH_3$ and ND_3.[137] The N in the clean TiN film comes exclusively from ammonia. Similarly, hydrogen in the gas-phase product, dimethylamine, also originates from ammonia. *In-situ* mass spectroscopic studies point out that the gas-phase transamination reaction yields high molecular weight clusters containing Ti, N, H, and perhaps C, which may be the intermediate responsible for the film growth. This intermediate has a high sticking coefficient, which leads to the poor step coverage observed on patterned SiO_2/Si substrates. Higher substrate temperatures would increase the surface mobility of the adsorbate but would also increase C incorporation into the film. On the other hand, the decomposition of the intermediate is thermally activated on the surface; thus, lowering the substrate temperature may decrease the reactive sticking coefficient and, consequently, improve the step coverage. These studies clearly have a significant contribution to make to the understanding and improvement of TiN CVD processes. Further, there are splendid opportunities for synthetic chemists to develop new precursors.

3.4. Nonthermal Processes in Semiconductor Etching

The increasing integration of microelectronics devices requires progressively more accurate pattern transfer, for which etching with high aspect ratio is critical. In the most common industrial processes, semiconductor etching is done in plasmas containing halogens (fluorine, chlorine, bromine). The introduction of these species and the processes they drive involve complex chemistry of a wide variety of neutrals and ions. Identifying key, rate-controlling steps and limiting undesirable processes certainly will be placed on a more reliable footing as the chemical

mechanisms and kinetics are characterized. The *advantage* of the plasma environment is the convenient nonthermal enhancement of the etch rate. The surface is exposed to nonthermally created chemical species (radicals, ions, photons, electrons, and translationally and/or internally excited neutrals), resulting in efficient etching. Also, in reactive ion etching, the electric field between the bulk of the plasma and the substrate accelerates the positively charged particles toward the substrate. This enhances the etch rate in the direction normal to the surface, which results in anisotropic etch profiles with high aspect ratio.[161−165] The disadvantage of reactive ion etching is that highly energetic particles, predominantly ions, present in the plasma damage the surface to an extent that may be detrimental to further structures (e.g., silicon oxide) later grown on the processed substrate.[166,167] Because of this, postetch treatment is frequently necessary to remove the near-surface defects before further processing. Improvement of the etch process is needed to better preserve the integrity of the substrate crystal structure during processing.[168]

The current surface chemical science efforts impacting etching have two main goals. (i) Obtain detailed understanding of the elemental processes occurring at the plasma−substrate interface. This is needed to help the engineering work whose goal is systematic development of plasma etch technology. (ii) Find chemical processes that are activated *nonthermally*. Such processes could lead to new etching methods that operate without plasma enhancement and have greater potential for anisotropic etching, which is desirable in a number of circumstances, for example, etching faster in a direction that deepens, rather than widens, a micron-sized trench. Thermally activated processes usually proceed in a directionally isotropic manner, and at high temperatures, sharp interfaces may be degraded by interdiffusion, damaging those structures prepared prior to the etch step.

With the methods of surface science, industrial etch processes can be modeled and studied under well-controlled laboratory conditions. In laboratory model systems a small number of reactions of a complex industrial etch process can be separated and studied *in situ*. Also, the elemental steps in a particular process, such as adsorption, migration on the surface, binding site and configuration, and formation and desorption of volatile compounds, can be studied systematically.[169−180] In this section we briefly review the fundamental chemical principles relevant to etching with particular emphasis on utilization of *nonthermal* methods in *anisotropic* processes. The cited references are intended only to illustrate the chemical principles. For more details, the reader is referred to recent, more comprehensive reviews on this topic.[163,164]

Anisotropic etching can be achieved by nonthermally activating the process in a particular (spatial) direction. The higher the degree of enhancement, the more anisotropic the etch process. The highest efficiency requires enhancement of the *rate-limiting step* of the chemical reaction. When trying to transfer results obtained with the tools of surface chemistry, typically in UHV, to the industrial processing environment, one has to know how the different environment influences the rate-limiting step. The rate-limiting step in an etch process may vary strongly with the reaction conditions, for example, a model for the chlorine/silicon etch system.[181,182] In this model, the rate-limiting step was assumed to be either the formation of weakly bound substrate−etchant compounds or the removal of these compounds from the surface. These rates are the function of such reaction parameters as the chemical nature (reactivity) of the etchant, the etchant flux (pressure), and the sample temperature.

In order to activate surface processes, energy must be delivered to the reaction interface. In a plasma this is accomplished by bombarding the surface with electrons, photons, and energetic (translational and/or internal) ions and neutrals. Most important is the effect of ions. Using model systems under UHV conditions, researchers have shown that Ar^+ bombardment in the case of the fluorine/silicon system substantially enhances the reaction rate[163] and activates etching of silicon with chlorine[183] and bromine,[184] processes which otherwise do not occur spontaneously at room temperature. This synergistic effect most likely accounts for the highly anisotropic etch rate in plasma-assisted etching. The dominant mechanism leading to such a synergistic effect is under debate.[161,162] One proposed mechanism is chemical sputtering, in which the role of the ions is to enhance the formation of volatile surface compounds, which then thermally desorb from the surface.[170] Another proposed mechanism is physical sputtering, in which the weakly bound surface compounds are sputtered away by the impact of the ions.[185,186] It has also been proposed that ion bombardment creates an open surface structure that is reactive in forming volatile surface compounds, which then desorb thermally.[161,162]

Photon activation of the etchant−substrate interaction is also being extensively studied. Although photons are present during plasma etching, the major reason for studying photoenhanced etching is that directed beams of photons could easily be introduced into etch systems to enhance anisotropy and avoid plasma excitation. The primary effect of continuous photon irradiation is an enhanced formation rate of highly volatile surface compounds: (Energetic) reactive radicals formed on the surface by photon irradiation interact with the surface more strongly than do the thermal etchant molecules. The volatile products desorb thermally.[187−190] Alternatively, photon-induced desorption of thermally stable surface compounds may also result in etching.[189] Photon irradiation by short energetic laser pulses may also enhance the etch rate by transient and very local surface heating.[189,191,192] Although the laser pulses in this case initiate thermal processes, etching is anisotropic, since heating occurs only on those surface areas that are in direct line of sight of the beam.

Recent studies have examined the enhancement of the etch rate with translationally and vibrationally hot etchant beams. Since these particles are present in plasmas in large quantities, understanding their interaction with the etched substrate is important.

Also, if molecular beam systems providing parallel beams of these particles were available, exposing the etched surface to such beams could result in anisotropic etching. The basic assumption here is that the excited reactive particles would lose their energy with high probability in the first collision with the surface, and the backscattered, less reactive particles would not etch the surface. This should lead to anisotropic etching on surface areas in direct line of sight with the primary beam.

As examples, enhanced etching of polysilicon with hot Cl_2[193] and SF_6[194] and of single crystalline silicon with chlorine trifluoride[195] has been demonstrated. A detailed study of Si(100) etching with hot atomic and molecular chlorine beams shows that translational excitation of atomic chlorine enhances the rate of volatile compound formation, and the impact of energetic particles in the beam initiates desorption of weakly bound surface species.[196] In the chlorine/Si(100) system, the etch rate was found to scale with the component of the kinetic energy normal to the surface. When the kinetic energy component of the chlorine atoms normal to the surface increased above 0.8 eV, the etch rate increased.[196] In the Cl_2/Si(100) system, the etch rate was enhanced when the beam contained chlorine molecules with kinetic energy above 6 eV.[197,198]

Vibrational excitation of the incident Cl_2 molecules produced minimal, if any, enhancement of the etch rate of Si(100).[198] The absence of any etching enhancement may be attributed to the limitation of thermal pumping of the vibrational levels prior to Cl_2 dissociation. However, enhanced etching of silicon, attributed to increased vibrationally hot SF_6, was observed when the SF_6 was thermally heated[194] and optically pumped[188] to high vibrational levels.

Finally, an example of anisotropic etching by a molecular beam by a thermal process was demonstrated.[199] Anisotropic etch profiles were observed when a Si(100) sample, held at $T \sim 1200$ K, was exposed to a collimated Cl_2 molecular beam. Since at this temperature molecular Cl_2 interacts with the silicon at a high rate, the anisotropic etch profile can be attributed to depletion of the primary beam. Under these conditions the reaction probability is high and the rate-limiting step is formation of volatile surface products, that is, limited by the etchant flux. No etch rate enhancement is expected by changing the properties of the incident molecules, and none was observed when the kinetic energy of the molecules in the beam was changed by He seeding.[199]

3.5. Summary

To summarize, even for highly developed silicon-based technologies which are, in many respects, mature, the technological goal of faster, less expensive, more reliable microelectronic devices and machines lead, quite naturally, to a broad range of surface and interface chemistry issues. Bandgap engineering through control of stoichiometry, a strong component of compound semiconductor research, shows up in silicon-based research as alloy compositional control, i.e., Si−Ge and Si−Ge−C alloys. The chemistry of hydrides on Si−Ge surfaces and its relation to film growth rates is a fascinating chemical kinetics question that is being probed by sophisticated tools of modern surface science including *in-situ* femtosecond second-harmonic generation. Chemical challenges include methods for preparing kinetically stabilized nonequilibrium alloy concentrations of carbon. As the layer thickness of dielectric materials, such as SiO_2, decreases into the 40 Å regime, the amount of bulk oxide becomes a small fraction of the total dielectric. Thus, defect and strain-related interface properties become critical. Empirically, nitriding is known to improve device performance; the chemical challenge is to characterize the role of nitrogen incorporation. Barrier layers, between semiconductors, insulators, and metals, play an ever-increasing role in the ultimate performance as device structures shrink in size into and below the 0.25 μm regime. Similarly, characteristics of conductive interconnects are crucial. The precursor surface chemistries of transition metal nitrides, useful as barrier layers, and of copper, useful as interconnects, serve as two technologically relevant and chemically challenging examples. Finally, even more chemical complexities, and fascinating reactivity and structural questions, are encountered in plasma-driven surface chemistry, a nonthermal process widely used in microelectronics manufacturing. Dissecting this complicated chemistry into parts that can be managed and treated at a fundamental molecular kinetics level is providing insights into the relative roles of the various modes of excitation and types of excited species that are present in plasmas.

4. Concluding Remarks

In this paper, we have illustrated, with several examples, the roles that surface chemistry plays and will play in thin film processing of semiconductor materials. Some areas are reasonably mature technologies, while others are newly emerging. Silicon-based technologies are the most fully developed, yet many present manufacturing processes involve chemical questions of mechanisms and kinetics that are, as yet, unresolved. This is particularly evident when the whole electronic device is considered, and it becomes clear that materials other than electronically active ones can have a major impact on device cost, reliability, and performance. In the present paper, the importance of oxynitrides as gate dielectrics, of TiN as a barrier layer, and of Cu as an interconnect material has been discussed with particular emphasis on the chemical issues involved. Building on a silicon base, there are yet many opportunities for chemistry in active materials, for example, Si−Ge alloys which are discussed here, as well as in Si−Ge−C alloys. Compound semiconductors, desirable as optoelectronic and high-speed conventional integrated circuit components, are much less highly developed areas, in part because their compound nature brings the challenging opportunity to control stoichiometry and alloy composition. Successfully realizing such control can lead to wavelength-tuned, i.e., bandgap-engineered, materials. In the case of III−V (13−15) compound semiconductors, opportunities abound for major contributions by synthetic chemists and surface chemists. In this paper, the

overview focuses on GaAs, but the future technological pull toward nitrides and antimonides is strong.

List of Acronyms Used

AES	Auger electron spectroscopy
ALE	atomic layer epitaxy
ARXPS	angle-resolved X-ray photoelectron spectroscopy
CBE	chemical beam epitaxy
CVD	chemical vapor deposition
FTIR	Fourier transform infrared
HREELS	high-resolution electron energy loss spectroscopy
MOCVD	metalloorganic chemical vapor deposition
MOMBE	metalloorganic molecular beam epitaxy
MOS	metal−oxide−semiconductor
PVD	physical vapor deposition
RDS	reflectance-difference spectroscopy
ROXNOX	reoxidation of nitrided oxide
RTP	rapid-thermal-process
SHG	second-harmonic generation
SSIMS	static secondary-ion mass spectroscopy
TPD	temperature-programmed desorption
ULSI	ultralarge scale integrated
UHV	ultrahigh vacuum
VLSI	very large scale integrated
XPS	X-ray photoelectron spectroscopy

Acknowledgments

Support of this work by the Science and Technology Centers program of the National Science Foundation and by the Center for Materials Chemistry of the University of Texas is gratefully acknowledged.

References

(1) Stringfellow, G. B. *Organometallic Vapor-Phase Epitaxy: Theory and Practice*; Academic Press, Inc.: San Diego, 1989.
(2) Deparis, C.; Massies, J. *J. Cryst. Growth* **1991,** *108*, 157
(3) Kamiya, I.; Aspnes, D. E.; Florez, L. T.; Harbison, J. P. *Phys. Rev.* **1992**, *B46*, 894.
(4) Heitzinger, J. M.; White, J. M.; Ekerdt, J. G. *Surf. Sci.* **1994,** *299/300*, 892.
(5) Creighton, J. R.; Banse, B. A. *Mater. Res. Soc. Symp. Proc.* **1991**, *222*, 15.
(6) Zhu, X.-Y.; White, J. M.; Creighton, J. R. *J. Vac. Sci. Technol.* **1992,** *A10*, 316.
(7) Yu, M. L.; Memmert, U.; Buchan, N. I.; Kuech, T. F. *Mater. Res. Symp. Proc.* **1991**, *204*, 37.
(8) Banse, B. A.; Creighton, J. R. *Surf. Sci.* **1991**, *257*, 221.
(9) Buchan, N. I.; Yu, M. L. *Surf. Sci.* **1993**, *280*, 383.
(10) Heitzinger, J. M.; Jackson, M. S.; Ekerdt, J. G. *Appl. Phys. Lett.* **1995,** *66*, 352.
(11) Yu, M. L.; Memmert, U.; Kuech, T. F. *Appl. Phys. Lett.* **1989,** *55*, 1011.
(12) Yu, M. L. *J. Appl. Phys.* **1993**, *73*, 716.
(13) Creighton, J. R. *Surf. Sci.* **1990**, *234*, 287.
(14) Murrell, A. J.; Wee, A. T. S.; Fairbrother, D. H.; Singh, N. K.; Foord, J. S. *J. Appl. Phys.* **1990,** *68*, 4053.
(15) Kuech, T. F.; Potemski, R. *Appl. Phys. Lett.* **1985**, *47*, 821.
(16) Putz, N.; Heinecke, H.; Heyen, M.; Balk, P.; Wayers, M.; Luth, H. *J. Cryst. Growth* **1986,** *74*, 292.
(17) Davison, P. J.; Lappert, M. F.; Pearce, R. *Chem. Rev.* **1976**, *76*, 219.
(18) Elschenbroich, C.; Salzer, A. *Organometallics*; VCH: Weinheim, 1979; p 13.
(19) Heitzinger, J. M.; Ekerdt, J. G. *J. Vac. Sci. Technol. A* **1995**, *13*, 2772.
(20) Keeling, L. A.; Chen, L.; Greenlief, C. M.; Mahajan, A.; Bonser, D. *Chem. Phys. Lett.* **1994**, *217*, 136.
(21) Creighton, J. R. *J. Vac. Sci. Technol.* **1990,** *A8*, 3984.
(22) Pütz, N.; Veuhoff, E.; Heinecke, H.; Heyen, M.; Lüth, H.; Balk, P. *J. Vac. Sci. Technol.* **1985,** *B3*, 671.
(23) Weyers, M.; Pütz, N.; Heinecke, H.; Heyen, M.; Lüth, H.; Balk, P. *J. Electron. Mater.* **1986,** *15*, 57.
(24) Abernathy, C. R.; Pearton, S. J.; Caruso, R.; Ren, F.; Kovalchik, J. *Appl. Phys. Lett.* **1989,** *55*, 1750.
(25) Abernathy, C. R.; Ren, F.; Pearton, S. J.; Song, J. *J. Electron. Mater.* **1992,** *21*, 323.
(26) Tu, C. W.; Liang, B. W.; Chin, T. P.; Zhang, J. *J. Vac. Sci. Technol.* **1990,** *B8*, 193.
(27) Sandhu, A.; Nakamura, T.; Ando, H.; Domen, K.; Okamoto, N.; Fujil, T. *J. Cryst. Growth* **1992,** *120*, 296.
(28) Mochizuki, K.; Ozeki, M.; Kodama, K.; Ohtsuka, N. *J. Cryst. Growth* **1988,** *93*, 557.
(29) Reid, K. G.; Urdianyk, H. M.; Bedair, S. M. *Appl. Phys. Lett.* **1991,** *59*, 2397.
(30) Chung, B.-C.; Green, R. T.; MacMillan, H. F. *J. Cryst. Growth* **1991,** *107*, 89.
(31) Dapkus, P. D.; Manasevit, H. M.; Hess, K. L.; Low, T. S.; Stillman, G. E. *J. Cryst. Growth* **1981,** *55*, 10.
(32) Kuech, T. F.; Veuhoff, V. *J. Cryst. Growth* **1984**, *68*, 148.
(33) Watkins, S. P.; Haacke, G. *Appl. Phys. Lett.* **1991,** *59*, 2263.
(34) (a) Creighton, J. R.; Bansenauer, B. A.; Huett, T.; White, J. M. *J. Vac. Sci. Technol.* **1993,** *A11* (4), 876. (b) Zhu, X.-Y.; White, J. M.; Creighton, J. R. *J. Vac. Sci. Technol.* **1992,** *A10*, 316.
(35) Stienstra, J.; Lewis, B. S.; Aarts, J. F. M. *J. Vac. Sci. Technol.* **1992,** *A10*, 920.
(36) Närmann, A.; Purtell, R. J.; Yu, M. L. *MRS Symp. Proc.* **1991,** *222*, 41.
(37) Luth, H.; Matz, R. *Phys. Rev. Lett.* **1981,** *46*, 1652.
(38) Dubois, L. H.; Schwartz, G. P. *Phys. Rev.* **1982,** *B26*, 794.
(39) Maslowski, E., Jr. *Vibrational Spectra of Organometallic Compounds*; John Wiley and Sons: New York, 1977; p 21.
(40) (a) Zhou, X.-L.; Zhu, X.-Y.; White, J. M. *Surf. Sci. Rep.* **1991,** *13*, 77. (b) White, J. M. *J. Vac. Sci. Technol.* **1992,** *B10*, 191.
(41) King, D. S.; Cavanagh, R. R. *Adv. Chem. Phys.* **1989,** *76*, 45.
(42) Doi, A.; Aoyagi, Y.; Namba, S. *Appl. Phys. Lett.* **1986**, *49*, 785.
(43) Chu, S. S.; Chu, T. L.; Chang, C. L.; Firouzi, H. *Appl. Phys. Lett.* **1988**, *52*, 1243.
(44) Maury, F.; Bouabid, K.; Fazouan, N.; Gue, A. M.; Esteve, D. *Appl. Surf. Sci.* **1995**, *86*, 447.
(45) Balk, P.; Fischer, M.; Grundmann, D.; Luckerath, R.; Luth, H.; Richter, W. *J. Vac. Sci. Technol.* **1987**, *B5*, 1453.
(46) Liu, H.; Roberts, J. C.; Ramdani, J.; Bedair, S. M.; Farari, J.; Vilcot, J. P.; Decoster, D. *Appl. Phys. Lett.* **1991,** *58*, 388.
(47) Zhu, X. Y.; Wolf, M.; White, J. M. *J. Chem. Phys.* **1992,** *97*, 605.
(48) McCaulley, J. A.; McCrary, V. R.; Donnelly, V. M. *J. Phys. Chem.* **1988,** *93*, 1148.
(49) Maayan, E.; Kreinin, O.; Veinger, D.; Thon, A.; BAhir, G.; Salzman, J. *J. Appl. Phys. Lett.* **1995,** *66*, 296.
(50) Shogen, S.; Ohashi, M.; Hashimoto, S.; Matsumi, Y. *Jpn. J. Appl. Phys.* **1993,** *32*, 3039.
(51) Cui, S.; Hacker, K.; Xin, Q.-S.; Hinton, R. A.; Zhu, X.-Y. *J. Phys. Chem.* **1995,** *99*, 11512.
(52) (a) Nakamura, S.; Mukai, T.; Senoh, M. *Jpn. J. Appl. Phys.* **1991**, *30*, L1998. (b) Nakamura, S.; Seno, M.; Nagahama, S.-I.; Iwasa, N.; Yamada, T.; Matsushita, T.; Kiyoku, H.; Sugimoto, Y. *Jpn. J. Appl. Phys.* **1996,** *35*, L74.
(53) (a) Neumayer, D. A.; Ekerdt, J. G. *Chem. Mater.* **1996**, *8*, 9. (b) Morkoc, H.; Mohammad, S. N. *Science* **1995**, *267*, 51. (c) Morkoc, H.; Strite, S.; Gao, G. B; Lin, M. E.; Sverdlov, B.; Burns, M. *J. Appl. Phys.* **1994**, *76*, 1363. (d) Strite, S.; Morkoc, H. *J. Vac. Sci. Technol. B* **1992**, *10*, 1237. (e) Matsuoka, T.; Ohki, T.; Ohno, T.; Kawaguchi, Y. *J. Cryst. Growth* **1994**, *138*, 727.
(54) Khan, M. A.; Kuznia, J. N.; Van Hove, J. M.; Olson, D. T. *Appl. Phys. Lett.* **1991**, *58*, 526.
(55) Zembutsu, S.; Sasaki, T. *J. Cryst. Growth* **1986**, *77*, 250.
(56) Sandroff, C. J.; Hedge, M. S.; Chang, C. C. *J. Vac. Sci. Technol.* **1989**, *B7*, 841.
(57) Shikata, O.; Hayashi, J. *J. Vac. Sci. Technol.* **1991**, *B9*, 2479.
(58) Zhu, X.-Y.; Wolf, M.; Huett, T.; White, J. M. *J. Chem. Phys.* **1992,** *97*, 5856.
(59) Ruckman, M.; Cao, W. J.; Park, K. T.; Gao, Y.; Wicks, G. W. *Appl. Phys. Lett.* **1991,** *59*, 849.
(60) Bu, Y.; Lin, M. C. *Surf. Sci.* **1994,** *317*, 152.
(61) (a) Sun, Y.-M.; Ekerdt, J. G. *J. Vac. Sci. Technol.* **1993,** *B11*, 610. (b) Sun, Y.-M.; Huett, T.; Sloan, D.; White, J. M.; Ekerdt, J. G. *Surf. Sci. Lett.* **1993**, *295*, L982.
(62) Nooney, M. G.; Liberman, V.; Martin, R. M. *J. Vac. Sci. Technol.* **1995,** *A13*, 1837.
(63) Yoshida, N.; Chichibu, S.; Akane, T.; Tosuka, M.; Uji, H.; Matsumoto, S. *Appl. Phys. Lett.* **1993,** *63*, 3035.
(64) Zavadil, K. R.; Ashby, C. I. H.; Howard, A. J.; Hommons, B. E. *J. Vac. Sci. Technol.* **1994,** *A12*, 1045.
(65) Bozos, F.; Avouris, Ph. *Phys. Rev. Lett.* **1986,** *57*, 1185.
(66) See the recent reviews: Mokler, S. M. *Crit. Rev. Surf. Chem.* **1994**, *4*, 1. Bean, J. C. *Proc. IEEE* **1992**, *80*, 571. Meyerson, B. S. *IBM J. Res. Dev.* **1990**, *34*, 806.
(67) Sturm, J. C.; Schwartz, P. V.; Prinz, E. J.; Manoharan, H. *J. Vac. Sci. Technol.* **1991,** *B9*, 2011.
(68) (a) Ning, B. M. H.; Crowell, J. E. *Appl. Phys. Lett.* **1992**, *60*, 2914. (b) Crowell, J. E.; Lu, G.; Ning, B. M. H. *Mater. Res. Soc. Symp. Proc.* **1991,** *204*, 253. (c) Ning, B. M. H.; Crowell, J. E. *Surf. Sci.* **1993**, *295*, 79.
(69) Klug, D. A.; Du, W.; Greenlief, C. M. *Chem. Phys. Lett.* **1992**, *197*, 352.

(70) (a) Tsu, R.; Lubben, D.; Bramblett, T. R.; Greene, J. E. *Thin Solid Films* **1993**, *225*, 191. (b) Suda, Y.; Lubben, D.; Matooka, T.; Greene, J. E. *J. Vac. Sci. Technol.* **1990**, *A8*, 61.
(71) (a) Gates, S. M.; Greenlief, C. M.; Beach, D. B.; Holbert, P. A. *J. Chem. Phys.* **1990**, *92*, 3144. (b) Jones, M. E.; Xia, L.-Q.; Maity, N.; Engstrom, J. R. *Chem. Phys. Lett.* **1994**, *229*, 401.
(72) (a) D'Evelyn, M. P.; Yang, Y. L.; Sutcu, L. F. *J. Chem. Phys.* **1992,** *96*, 852; (b) D'Evelyn, M. P.; Cohen, S. M.; Rouchouze, E.; Yang, Y. L. *J. Chem. Phys.* **1993,** *98*, 3560.
(73) Jang, S.-M.; Reif, R. *Appl. Phys. Lett.* **1992,** *60*, 707.
(74) Jang, S.-M.; Reif, R. *Appl. Phys. Lett.* **1991,** *59*, 707.
(75) Russell, N. M.; Breiland, W. G. *J. Appl. Phys.* **1993,** *73*, 3525.
(76) Eres, G.; Sharp, J. W. *J. Appl. Phys.* **1993,** *74*, 7241.
(77) Höfer, U.; Li, L.; Heinz, T. F. *Phys. Rev.* **1992,** *B45*, 9485.
(78) Flowers, M. C.; Jonathan, N. B. H.; Liu, Y.; Morris, A. *J. Chem. Phys.* **1993,** *99*, 7038.
(79) Mokler, S. M.; Ohtani, N.; Xie, M. H.; Zhang, J.; Joyce, B. A. *Appl. Phys. Lett.* **1992,** *61*, *2548*.
(80) Garone, P. M.; Strum, J. C.; Schwartz, P. V.; Schwarz, S. A.; Wilkens, B. J. *Appl. Phys. Lett.* **1990,** *56*, 1275.
(81) Meyerson, B. S.; Uram, K. J.; LeGoues, F. K. *Appl. Phys. Lett.* **1988,** *53*, 2555.
(82) Russell, N. M.; Ekerdt, J. G. Manuscript in preparation.
(83) McGilip, J. F. *Prog. Surf. Sci.* **1995,** *49*, 1.
(84) Shen, Y. R. *Principles of Nonlinear Optics*; Wiley: New York, 1984.
(85) Heinz, T. F. In *Nonlinear Surface Electromagnetic Phenomena*; Ponath, H.-E., Stegeman, G. I., Eds.; North-Holland: Amsterdam, 1991.
(86) Bloembergen, N.; Pershan, P. S. *Phys. Rev.* **1962,** *128*, 606.
(87) Sipe, J. E.; Moss, D. J.; van Driel, H. M. *Phys. Rev.* **1987,** *B35*, 1129.
(88) Lüpke, G.; Bottomley, D. J.; van Driel, H. M. *Phys. Rev.* **1993,** *B47*, 10389.
(89) Bjorkman, C. H.; Yasuda, T.; Shearon, C. E., Jr.; Ma, Y.; Lucovsky, G.; Emmerichs, U.; Meyer, C.; Leo, K.; Kurz, H. *J. Vac. Sci. Technol.* **1993,** *B11*, 1521.
(90) Daum, W.; Krause, H.-J.; Reichel, U.; Ibach, H. *Phys. Rev. Lett.* **1993,** *71*, 1234.
(91) Tom, H. W. K.; Heinz, T. F.; Shen, Y. R. *Phys. Rev. Lett.* **1983,** *51*, 1983.
(92) Heinz, T. F.; Loy, M. M. T.; Thompson, W. A. *Phys. Rev. Lett.* **1985,** *54*, 63.
(93) Suzuki, T.; Hirabyashi, Y. *Jpn. J. Appl. Phys., Part 2* **1993,** *32*, L610.
(94) Hollering, R. W. J.; Hoeven, A. J.; Lenssinck, J. M. *J. Vac. Sci. Technol.* **1990,** *A8*, 3194.
(95) McGilip, J. F.; Yeh, Y. *Solid State Commun.* **1986,** *59*, 91.
(96) Kelly, P. V.; O'Mahony, J. D.; McGilip, J. F.; Rasing, Th. *Appl. Surf. Sci.* **1992,** *56*−*58*, 453.
(97) Power, J. R.; McGilip, J. F. *Surf. Sci.* **1994**, *307*/*309*, 1066.
(98) Hollering, R. W. J.; Dijkkamp, D.; Lindelauf, H. W. L.; van der Heide, P. A. M.; Krijin, M. P. C. M. *J. Vac. Sci. Technol.* **1990,** *A8*, 3997.
(99) Kelly, P. V.; Tang, Z.-R.; Woolf, D. A.; Williams, R. H.; McGilip, J. F. *Surf. Sci.* **1991,** *251*/*252*, 87.
(100) Pedersen, K.; Morgen, P. *Phys. Scrip.* **1994**, *T54*, 238.
(101) Heinz, T. F.; Loy, M. M. T.; Iyer, S. S. *Mater. Res. Symp. Proc.* **1987**, *75*, 697.
(102) Sakamoto, K.; Sakamoto, T.; Nagao, S.; Hashiguchi, G.; Kuniyoshi, K.; Bando, Y. *J. Appl. Phys.* **1987**, *26*, 666.
(103) Dadap, J. I.; Russell, N.; Hu, X. F.; Ekerdt, J.; Downer, M. C. *SPIE* **1994**, *2337*, 68.
(104) Ting, W.; Lo, G. Q.; Ahn, J.; Chu. T.; Kwong, D. L. *Proc. IEEE Reliability Phys. Symp.* **1991,** 323.
(105) Hori, T.; Iwasaki, H.; Tsuji, K. *IEEE Trans. Electron Devices* **1989**, *36*, 340.
(106) Govorkov, S. V.; Emel'yanov,V. I.; Koroteev, N. I.; Petrov, G. I.; Shumay, I. L.; Yakovlev, V. V. *J. Opt. Soc. Am.* **1989,** *B6*, 1117.
(107) McGilp, J. F.; Cavanagh, M.; Power, J. R.; O'Mahony, J. D. *Appl. Phys.* **1994,** *A59*, 401.
(108) Meyer, C.; Lüpke, G.; Emmerichs, U.; Wolter, F.; Kurz, H.; Bjorkman, C. H.; Lucovsky, G. *Phys. Rev. Lett.* **1995,** *74*, 3001.
(109) Emmerichs, U.; Meyer, C.; Bakker, H. J.; Kurz, H.; Bjokman, C. H.; Shearon, C. E.; Ma, Y.; Yasuda, T.; Jing, Z.; Lucovsky, G.; Whitten, J. L. *Phys. Rev.* **1994,** *B50*, 5506.
(110) Meyer, C.; Lüpke, G.; Emmerichs, U.; Wolter, F.; Kurz, H.; Bjorkman, H.; Lucosky, G. *Phys. Rev. Lett.* **1995**, *74*, 3001.
(111) Dadap, J. I.; Doris, B.; Deng, Q.; Downer, M. C.; Lowell, J. K.; Diebold, A. C. *Appl. Phys. Lett.* **1994,** *64*, 2139.
(112) Dunn, G. J.; Scott, S. *IEEE Trans. Electron Devices* **1990**, *37*, 1719.
(113) Dunn, G. J.; Krick, J. T. *IEEE Trans. Electron Devices* **1991**, *38*, 901.
(114) Momose, H. S.; Morimoto, T.; Wzawa, Y.; Tsuchiaki, M.; Ono, M.; Yamabe, K.; Iwai, H. *Extended Abstr. IEEE Int. Electron Device Meeting* **1991**, 359.
(115) Hwang, H.; Ting, W.; Kwong, D. L.; Lee, J. *IEEE Electron Device Lett.* **1991,** *EDL-12*, 495.
(116) Okada, Y.; Tobin, P. J.; Rushbrook, P.; DeHart, W. L. *IEEE Trans. Electron Devices* **1994**, *41*, 191.
(117) Liu, Z. H.; Krick, J. T.; Wann, H. J.; Ko, P. K.; Hu, C.; Cheng, Y. C. *IEDM Technol. Dig.*, **1992**, 625.
(118) Woerlee, P. H.; Lifka, H.; Montree, A. H.; Paulzen, G. M.; Pomp, H.; Woltjer, R. *Int. Symp. VLSI Technol.* **1993**, 105.
(119) Lo, G. Q.; Ting, W.; Ahn, J.; Kwong, D. L. *IEEE Trans. Electron Device Lett.* **1992,** *EDL13*, 111.
(120) Okada, Y.; Tobin, P. J.; Reid, K. G.; Hegde, R. I.; Maiti, B.; Ajuria, S. A. *Technol. Dig. Symp. VLSI Technol.* **1994**, 105.
(121) Heremans, P.; Bellens, R.; Groeseneken, G.; Maes, H. E. *IEEE Trans. Electron Devices* **1988**, *35*, 2194.
(122) Bhat, M.; Kim, J.; Yan, J.; Yoon, G. W.; Han, L. K.; Kwong, D. L. *IEEE Electron Device Lett.* **1994**, *EDL-13*, 421.
(123) Briner, E.; Meiner, Ch.; Rothen, A. *J. Chim. Phys.* **1926**, *23*, 609.
(124) Banerjee, I.; Kuzminov, D. *J. Vac. Sci. Technol.* **1994**, *B12*, 205.
(125) Hori, T.; Iwasaki, H.; Tsuji, K. *IEEE Trans. Electron Devices* **1989,** *36*, 340.
(126) Fukuda, H.; Yasuda, M.; Iwabuchi, T.; Ohno, S. *IEEE Electron Device Lett.* **1991**, *EDL-12*, 587.
(127) Sun, S. C.; Plummer, J. D. *IEEE Trans. Electron Devices* **1980**, *27*, 1497.
(128) Hori, T. *IEEE Trans. Electron Devices* **1990**, *37*, 1058.
(129) Bhat, M.; Wristers, D. J.; Han, L.-K.; Yan, J.; Fulford, H. J.; Kwong, D. L. *IEEE Trans. Electron Devices* **1995**, *42*, 907.
(130) Yoon, G. W.; Joshi, A. B.; Kim, J.; Kwong, D. L. *IEEE Electron Device Lett.* **1993**, *14*, 179.
(131) Fang, H.; Krisch, K. S.; Gross, B. J.; Sodini, C. G.; Chung, J.; Antoniadis, D. A. *IEEE Trans. Electron Devices* **1992**, *13*, 217.
(132) Okada, Y.; Tobin, P. J.; Hegde, R. *Appl. Phys. Lett.* **1992**, *61*, 3163.
(133) Liu, Z.; Wann, H. J.; Ko, P. K.; Hu, C.; Cheng, Y. C. *IEEE Electron Device Lett.* **1992**, 519.
(134) Bhat, M.; Kamath, A.; Kwong, D. L.; Sun, Y. M.; White, J. M. *Appl. Phys. Lett.* **1994**, *65*, 1314.
(135) Lutz, F.; Bischoff, J. L.; Kubler, L.; Bolmont, D. *Appl. Surf. Sci.* **1993**, *73*, 427.
(136) Rangelov, G.; Stober, J.; Eisenhut, B.; Fauster, Th. *Phys. Rev. B* **1991**, *44*, 1954.
(137) Nishijima, M.; Kobayashi, H.; Edamoto, K.; Onchi, M. *Surf. Sci.* **1984**, *137*, 473.
(138) Chu, T. Y.; Ting, W.; Ahn, J. H.; Lin, S.; Kwong, D. L. *Appl. Phys. Lett.* **1991**, *59*, 1412.
(139) Wang, S.-Q. *MRS Bull.* **1994,** August, 31.
(140) Li, J.; Shacham-Diamand, Y.; Mayer, J. W. *Mater. Sci. Rep.* **1992,** *9*, 11.
(141) Arita, Y. *Semiconductor World* **1993**, December, 158.
(142) Li, J.; Seidel, T. E.; Mayer, J. W. *MRS Bull.* **1994**, August, 15.
(143) Harper, J. M. E.; Colgan, E. G.; Hu, C.-K.; Hummel, J. P.; Buchwalter, L. P.; Uzoh, C. E. *MRS Bull.* **1994**, August, 23.
(144) Choi, C. S.; Ruggles, G. A.; Shah, A. S.; Xing, G. C.; Osburn, C. M.; Hunn, J. D. *J. Electrochem. Soc.* **1991**, *138*, 30622.
(145) Chang, C.-A. *J. Vac. Sci. Technol.* **1990**, *A8*, 3796.
(146) Chittipeddi, S.; Kelly, M. J.; Dziuba, C. M.; Oales, A. S.; Cochran, W. T. *Mater. Res. Soc. Symp. Proc.* **1990**, *181*, 527.
(147) Russell, S. W.; Li, J.; Strane, J. W.; Mayer, J. W. *Mater. Res. Soc. Symp. Proc.* **1992,** *265*, 205.
(148) Creighton, J. R.; Parmeter, J. E. *Crit. Rev. Solid State Sci.* **1993**, *18*, 175.
(149) Doppelt, P.; Baum, T. H. *MRS Bull.* **1994,** *19*, 41.
(150) Gelatos, A. V.; Jain, A.; Marsh, R.; Mogab, C. J. *MRS Bull.* **1994**, *19*, 49.
(151) Jain, A.; Chi, K.-M.; Kodas, T. T.; Hampden-Smith, M. J. *J. Electrochem. Soc.* **1993**, *140*, 1434.
(152) Dubois, L. H.; Zegarski, B. R. *J. Electrochem. Soc.* **1992**, *139*, 3295.
(153) Jain, A.; Chi, K.-M.; Hampden-Smith, M. J.; Kodas, T. T.; Farr, J. D.; Paffett, M. F. *J. Mater. Res.* **1992**, *7*, 261.
(154) Cohen, S. L.; Liehr, M.; Kasi, S. *Appl. Phys. Lett.* **1992**, *60*, 1585.
(155) Shin, H.-K.; Chi, K.-M.; Hampden-Smith, M. J.; Kodas, T. T.; Farr, J. D.; Paffett, M. F. *Adv. Mater.* **1991**, *3*, 246.
(156) Jain, A.; Chi, K.-M.; Kodas, T. T.; Hampden-Smith, M. J.; Farr, J. D.; Paffett, M. F. *Chem. Mater.* **1991**, *3*, 995.
(157) Cheng, H.-E.; Chiang, M.-J.; Han, M.-H. *J. Electrochem. Soc.* **1995**, *142*, 1573.
(158) Yokoyama, N.; Hindo, K.; Homma, Y. *J. Electrochem. Soc.* **1991**, *138*, 190.
(159) Dubois, L. H.; Zegarski, B. R.; Girolami, G. S. *J. Electrochem. Soc.* **1992**, *139*, 3603.
(160) Prybyla, J. A.; Chiang, C.-M.; Dubois, L. H. *J. Electrochem. Soc.* **1993**, *140*, 2695.
(161) Flamm, D. L.; Donnelly, V. M.; Ibbotson, D. E. *J. Vac. Sci. Technol.* **1983,** *B1*, 23.
(162) Winters, H. F.; Coburn, J. W.; Chuang, T. J. *J. Vac. Sci. Technol.* **1983,** *B1*, 469.
(163) Winters, H. F.; Coburn, J. W. *Surf. Sci. Rep.* **1992,** *14*, 161.
(164) Yu, M. L.; DeLouise, L. A. *Surf. Sci. Rep.* **1993**, *19*, 285.
(165) Coburn, J. W. *Appl. Phys.* **1994,** *A59*, 451.
(166) Connick, I.-H.; Bhattacharyya, A.; Ritz, K. N.; Smith, W. L. *J. Appl. Phys.* **1988,** *64*, 2059.

(167) Sung, K. T.; Pang, S. W. *J. Vac. Sci. Technol.* **1994,** *A12*, 1346.
(168) *Plasma Processing of Materials: Scientific Opportunities and Technological Challenges*; National Research Council, National Academy Press: Washington, DC, 1991.
(169) Gupta, P.; Coon, P. A.; Koehler, B. G.; George, S. M. *Surf. Sci.* **1991,** *249*, 92.
(170) Whitman, L. J.; Joyce, S. A.; Yarmoff, J. A.; McFeely, F.; Terminello, L. J. *Surf. Sci.* **1990,** *232*, 297.
(171) Schnell, R. D.; Rieger, D.; Bogen, A.; Himpsel, F. J.; Wandelt, K. *Phys. Rev.* **1985**, *B32*, 8057.
(172) Matsuo, J.; Karahashi, K.; Sato, A.; Hijiya, S. *Jpn. J. Appl. Phys., Part 1* **1992,** *31*, 2025.
(173) Craig, B. I.; Smith, P. V. *Surf. Sci.* **1992,** *262*, 235.
(174) Gao, Q.; Cheng, C. C.; Chen, P. J.; Choyke, W. J.; Yates, J. T. *J. Chem. Phys.* **1993,** *98*, 8308.
(175) Boland, J. J.; Villarubia, J. S. *Phys. Rev.* **1990,** *B41*, 9865.
(176) Etelaniemi, V.; Michel, E. G.; Materlik, G. *Surf. Sci.* **1991,** *251/252*, 483.
(177) Sullivan, D. J. D.; Flaum, H. C.; Kummel, A. C. *J. Phys. Chem.* **1993**, *97*, 12051.
(178) Johansson, L. S. O.; Uhrberg, R. I. G.; Lindsay, R.; Wincott, P. L.; Thornton, G. *Phys. Rev.* **1990**, *B42*, 9534.
(179) Mendicino, M. A.; Seebauer, E. G. *Appl. Surf. Sci.* **1993,** *68*, 285.
(180) Szabo, A.; Farral, P. D.; Engel, T. *Surf. Sci.* **1993**, *312*, 284.
(181) Szabo, A.; Engel, T. *J. Vac. Sci. Technol.* **1994,** *A12*, 648.
(182) Su, C.; Xi, M.; Dai, Z. G.; Vernon, M. F.; Bent, B. F. *Surf. Sci.* **1993,** *282*, 357.
(183) Chuang, M.; Coburn, J. W. *J. Vac. Sci. Technol.* **1990,** *A8*, 1969.
(184) Tyrrell, G. C.; Boyd, I. W.; Jackman, R. B. *Appl. Surf. Sci.* **1989,** *43*, 439.
(185) Dieleman, J.; Sanders, F. H. M.; Kolfschoten, A. W.; Zalm, P. C.; de Vries, A. E.; et al. *J. Vac. Sci. Technol.* **1985,** *B3*, 1384.
(186) Sanders, F. H. M.; Kolfschoten, A. W.; Dieleman, J.; Haring, R. A.; Haring, A.; et al. *J. Vac. Sci. Technol.* **1984,** *A2*, 487.
(187) Okano, H.; Horike, Y.; Sekine, M. *Jpn. J. Appl. Phys.* **1985,** *24*, 68.
(188) Chuang, T. J. *J. Chem. Phys.* **1981,** *74*, 1453.
(189) Sesselmann, W.; Hudeczek, E.; Bachmann, F. *J. Vac. Sci. Technol.* **1989,** *B7*, 1284.
(190) Baller, T. S.; Kools, J. C. S.; Dieleman, J. *Appl. Surf. Sci.* **1990,** *46*, 292.
(191) Boulmer, J.; Bourguignon, B.; Budin, J. P.; Däbarre, D.; Desmur, A. *J. Vac. Sci. Technol.* **1991,** *A9*, 2923.
(192) Baller, T.; Costra, D. J.; de Vries, A. E.; van Veen, G. N. A. *J. Appl. Phys.* **1986,** *60*, 2321.
(193) Suzuki, K.; Hiraoka, S.; Nishimatsu, S. *J. Appl. Phys.* **1988,** *64*, 3697.
(194) Suzuki, J.; Ninomiya, K.; Nishimatsu, S.; Okada, O. *Jpn. J. Appl. Phys.* **1986,** *25*, L373.
(195) Saito, Y.; Hirabaru, M.; Yoshida, A. *J. Vac. Sci. Technol.* **1992,** *B10*, 175.
(196) Szabo, A.; Farral, P. D.; Engel, T. *J. Appl. Phys.* **1993**, *75*, 3623.
(197) Campos, F. X.; Weaver, G. C.; Waltman, C. J.; Leone, S. R. *J. Vac. Sci. Technol.* **1992,** *B10*, 2217.
(198) Leone, S. R. *Jpn. J. Appl. Phys., Part 1* **1995,** *34*, 2073.
(199) Teraoka, Y.; Uesugi, F.; Nishiyama, I. In *Photons and Low Energy Particles in Surface Processing*; Ashby, C., Brannon, J. H., Pang, S., Eds.; Materials Research Society: Pittsburgh, 1992; pp 183.

CR950236Z